Received July 18, 2021, accepted August 18, 2021, date of publication August 24, 2021, date of current version September 2, 2021.

Digital Object Identifier 10.1109/ACCESS.2021.3107405

Analysis of a Mathematical Model for Drilling System With Reverse Air Circulation by Using the ANN-BHCS Technique

ASHFAQ AHMAD[1], MUHAMMAD SULAIMAN[1], POOM KUMAM[2,3,4], (Member, IEEE), MAHARANI ABU BAKAR[5], AND MIFTAHUDDIN[6]

[1]Department of Mathematics, Abdul Wali Khan University Mardan, Mardan, Khyber Pakhtunkhwa 23200, Pakistan
[2]KMUTT Fixed Point Research Laboratory, SCL 802 Fixed Point Laboratory, KMUTT-Fixed Point Theory and Applications Research Group, Department of Mathematics, Faculty of Science, King Mongkut's University of Technology Thonburi (KMUTT), Thung Khru, Bangkok 10140, Thailand
[3]Center of Excellence in Theoretical and Computational Science (TaCS-CoE), King Mongkut's University of Technology Thonburi (KMUTT), Thung Khru, Bangkok 10140, Thailand
[4]Department of Medical Research, China Medical University Hospital, China Medical University, Taichung 40402, Taiwan
[5]Faculty of Ocean Engineering Technology and Informatics, Universiti Malaysia Terengganu, Kuala Nerus, Kuala Terengganu 21300, Malaysia
[6]Department of Statistics, Faculty of Mathematics and Natural Sciences, Universitas Syiah Kuala, Banda Aceh 23111, Indonesia

Corresponding authors: Muhammad Sulaiman (msulaiman@awkum.edu.pk) and Poom Kumam (poom.kum@kmutt.ac.th)

This work was supported by the Center of Excellence in Theoretical and Computational Science (TaCS-CoE), King Mongkut's University of Technology Thonburi (KMUTT).

ABSTRACT In the present article, mathematical analysis of drilling system with reverse air circulation is presented by a novel hybrid technique of feedforward artificial neural network (ANN) and biogeography based cuckoo search (BHCS) algorithm. A series solution is constructed with unknown weights for the differential equations representing the drilling problem. Five numerical cases are analysed to show the effectiveness of our method for the solution of differential equations. From the experimental outcomes, it is investigated that our soft computing procedure has a better rate of convergence to the best solution as compared to state-of-the-art techniques. From solution graphs, it is established that our results are in agreement with the reference solutions. It is noted that our technique is easy to implement and can be used for any mathematical model containing nonlinear differential equations. The graphical abstract of this article is given in Figure (1).

INDEX TERMS Optimization problems, mathematical models, heuristics, artificial neural networks, drilling problem.

I. INTRODUCTION

In the technology of drilling air or different gases are used evacuation fluids to bring the cutting particles formed as a result of drilling at the lowest end of the borehole out to the surface. The technology is in use since the 1950s [1]. It improves the penetration rate in hard formation [2] and points out the problems of loss during circulation in naturally fractured and depleted reservoirs [3]–[6]. There are two kinds of techniques that are used in air and gas drilling. In the field of petroleum engineering; direct and reverse circulation is used for drilling. In straight boreholes, the reverse circulation technique is used for drilling. Compressed air is utilized as a mean of drilling fluid in this method, see Figure. (3). The compressed air is injected into the top of the annulus between the two walls of the drilling pipe, the air flows in annulus towards the lowest end of the borehole, the cutting particles at the lowest end of the borehole enter into compressed air and the compressed air brings the cutting particles up to the surface [7]. One of the advantages of this method is that the rock cuttings are continuously returned to the surface. It means that the system of reverse air circulation drilling is a closed system. Therefore, the volume of injected compressed air is proportional to the velocity of the air [8]. The efficiency of reverse circulation of air in drilling depends on whether the cutting particles can be shifted or not from the bottom to the central channel then up to the surface. The air's velocity must satisfy the demands of continuous returning of cutting

The associate editor coordinating the review of this manuscript and approving it for publication was Aniruddha Datta.

particles to clean the lowest end of the borehole. Therefore, it is very useful to discuss the velocity of the cutting particles during the drilling process.

The motion of the cutting particles in direct air circulation and gas drilling has already been studied by researchers [9]–[13]. In this drilling technique, the cutting particles are brought up to the surface from the bottom through the annular region between the walls of the well bore and the drill string. The cutting particles weaken the wall of the well bore that causes the instability of well bore [14]–[19]. The demand of airflow rate is large to keep clean the lowest end of the borehole as the cross-sectional area of the annular region is large that increases the drilling cost. The method of reverse air circulation is free from these problems as in this method the cutting particles are carried out to the surface through the drill pipe of dual walls. In this method, the velocity of air is larger than the velocity in other methods with the same volume of air injection because the dual wall drill pipe has a smooth surface and small cross-sectional area.

However, there still exist some problems. In the method of reverse air circulation, the drilling bit has some particular structure. Some researchers, like Bulroc and Numa, have primarily focussed on external jetting nozzles [20], [21]. Meanwhile, some studies have concentrated on bottom jetting nozzle bits [22]. The velocity of air is high because it flows through the nozzles of the bit to the lowest end of the borehole. Initially, the cutting particles sit still, and then with the help of aerodynamic drag force it starts to move. When the sliding frictional force controls the aerodynamic force, the particles remain motionless. In a situation, when the particles of compressed air are too large, its velocity is very low. It is impossible to change the bit's structure in order to obtain the smaller sizes of the particles and it is difficult to increase the volume of injected air to increase the velocity of the air, because the air compressor has limited workability. Thus, the breaking of the particle is repeated until its size is small enough to carry it out to the surface. Repeating the breaking of the particle wastes a lot of energy.

If the bits are of different structures then the size of the particles will be different [23]. If the particles have different sizes then the velocity of air, to keep clean the lowest part of the borehole, will also be different. Thus, the volume of air injection will be different. The compressibility of the air because of an increase in the depth of the borehole gradually decreases the volume of air injection [24]. In addition, the volume of the air also changes gradually as it returns. As the air velocity is changed, it affects the capacity of compressed air used to carry the cutting particles out to the surface. Hence, it is beneficial to analyze the motion of cutting particles to design the bit's structure and volume of air injection. These factors can help keep the lower end of the borehole clean and avoid the repetition in the breaking of particles.

The dilute phase pneumatic conveying process is involved in the motion of the cutting particles [8], [25], [26]. In the operations of reverse air circulation, single-phase flow involves the fluid flow from the top of the annular region to the lowest end of the borehole. Two-phase flow occurs when the fluid flow entrains the cuttings formed at the end of the borehole.

Hence, various soft computing approaches have been implemented for the solution of different real-life problems [27]–[38], [38]–[50]. Furthermore, analog active filter design, mathematical models of orthopedic implants, CMOS ring oscillation model, analysis of drilling parameters based on Pareto optimality are discussed and investigated in [51]–[55]. Mathematical models of drilling processes are analysed by many researchers by applying soft computing techniques such as Genetic Algorithm (GA), Ant Colony Optimization (ACO), Particle Swarm Optimization (PSO), Cuckoo Search (CS), Tabu Search (TS), Intelligent Water Drop (IWD), Swarm Intelligent (SI), Artificial intelligence (AI), Firefly Algorithm (FA) and some modified and hybrid approaches. A review of the soft computing approaches used for calculating solutions to drilling problems is given in Table (1). Exploration and exploitation are two essential characteristics of any metaheuristic for a balanced search in the search domain. Many of the researchers have proposed hybrids of these heuristics for a balanced search. Most of these hybrids fail to tackle problems involving complex objective functions with no prior information about their landscapes. Exploration and exploitation are two essential characteristics of any metaheuristic for a balanced search in the search domain. Many of the researchers have proposed hybrids of these heuristics for a balanced search. Most of these hybrids fail to tackle problems involving complex objective functions with no prior information about their landscapes [56].

Keeping in view the work done on the analysis of the drilling problem, the authors of this manuscript were interested in designing a better soft computing approach that can handle mathematical models representing real-life problems with ease of implementation and minimum effort with less arbitrary parameter settings.

This paper has studied the mathematical modeling of the velocity of cutting particles in a radial direction. The effects of air velocity and the size of the particle are considered in this model. The model was solved analytically by Zhu *et al.* [24]. We have designed a hybrid of Artificial Neural Networks (ANNs) and BHCS algorithm, named the ANN-BHCS algorithm. The ANN-BHCS algorithm solves the model, and the results are compared with other state-of-the-art approaches.

II. BASIC ASSUMPTIONS

The lowest end of the borehole is a confined circular space because the drill bit has a particular structure. Along the circumferential direction of the bottom of the borehole, various breaking points are found whose number depends on the number of the cutting teeth of the bit. The height from the bit's cutting face to the end of the borehole is not longer than the cutting tooth, and at the breaking point, a single particle of cutting rocks is accommodated. The Particle that is driven by the flow of air and slowed down due to sliding frictional force moves from the point where it breaks to the inlet of the central channel. As the bit operates, the particles of the cutting rocks are continuously stored in the inlet and move up from the central channel to the surface. That motion of the particles from a point where they break, to the inlet is called motion in the radial direction.

On the basis of technical features of the drilling with the reverse circulation of air, a single particle of the cutting rocks in the radial direction is considered as a research object. Perfect gas law can be used to approximate compressible air. Furthermore, in the drilling with straight boreholes, the cutting particles are uniformly distributed in the compressed air when they get into compressible air [26]. The rotation and the temperature of the drill pipe do not affect the flow field of the borehole. Moreover, the terminal effects of the particles and the drilling structures are not considered [57], [58].

III. DERIVATIONS

A. EQUIVALENT DIAMETER

The particles of cutting rocks have different shapes on the basis of some factors such as the bit's structure, condition of formation and rotary drilling circulation medium, etc. It is difficult to derive the mathematical form of the particle's motion, so we assume all the particles to be spherical. The particle's diameter based on the equivalent volume is calculated as:

$$d_{sv} = (6V_s/\pi)^{1/3}, \tag{1}$$

where d_{sv} and V_s represent the diameter and volume of the particle, respectively.

B. MODELLING THE PARTICLE'S MOTION IN RADIAL DIRECTION

Considering single particle in the radial direction, we concentrate on the case where drag force controls the sliding frictional force and the particle moves in the radial direction from the breaking point into the central channel (Fig.2). In the radial direction, the aerodynamic drag force F_d is

$$F_d = C_D A_r \rho_g \frac{(v_g - v_s)^2}{2}, \tag{2}$$

where C_D, A_r, ρ_g, v_g, and v_s are drag coefficients, the projected area of the particle, the density of air, velocities of air and particle, respectively.

The particle weight G_s is given as:

$$G_s = m_s g = \rho_s V_s g = \frac{\pi}{6} g \rho_s d_{sv}^3, \tag{3}$$

where m_s, ρ_s, and g denote the mass of the particle, density of the particle, and gravitational acceleration respectively. The frictional coefficient and weight of the particle determine the sliding frictional force. Here, the mathematical form of frictional force f_r is given as:

$$f_r = \mu_r G_s = \frac{\pi}{6} g \mu_r \rho_s d_{sv}^3, \tag{4}$$

TABLE 1. Review of soft computing approaches used in drilling processes.

Algorithm	Reference	SO	MO	Optimize travel distance	Reducing machining time	Minimizing cost	Improving efficiency	Increasing productivity
CS	[59]		✓		✓	✓	✓	
	[60]		✓	✓	✓			
TS	[61]	✓						✓
	[62]		✓		✓	✓		
GA	[63]	✓		✓				
	[64]	✓						✓
	[65]	✓			✓			
	[66]		✓		✓	✓	✓	
HA	[67]	✓			✓			
	[68]	✓			✓			✓
	[69]		✓				✓	✓
MA	[70]	✓		✓	✓			✓
	[71]	✓						✓
	[72]		✓	✓	✓			
IWD	[73]	✓		✓				
SI	[74]		✓	✓	✓			
AI	[75]	✓		✓				
FF	[76]	✓		✓				
MOA	[77]	✓		✓				
FL	[78]	✓				✓		

where μ_r is the coefficient of friction of cuttings at the lowest end of the borehole. Using Eqs. (2 and 4), we obtain the relationship of the critical diameter d_{cd} of the particle and

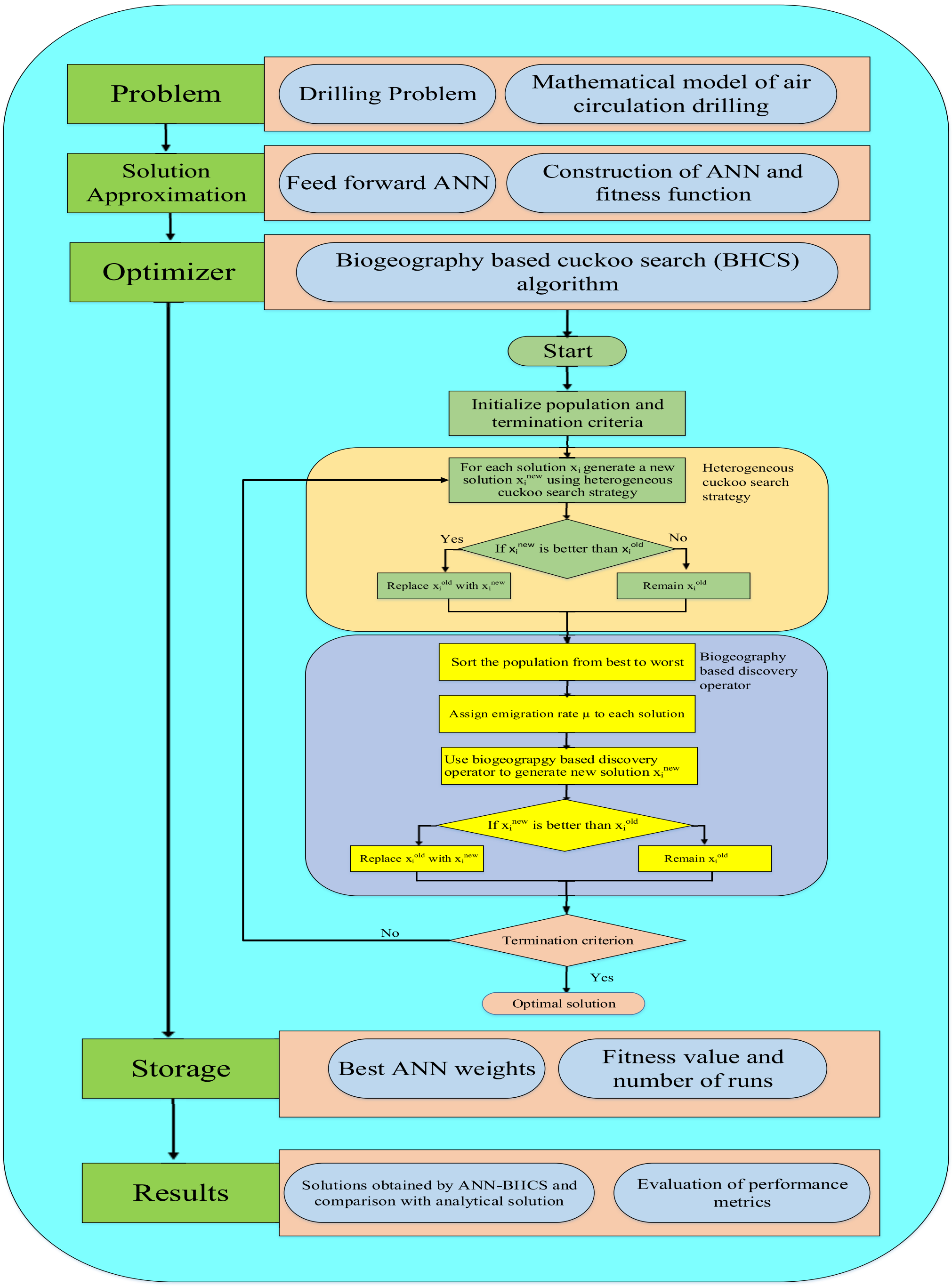

FIGURE 1. **Graphical illustration of the soft computing procedure followed in this paper.**

the critical velocity v_{cv} of compressed air at the end of the borehole as

$$C_D A_r \rho_g \frac{v_{cv}^2}{2} = C_D \rho_g \left(\frac{\pi}{4} d_{cd}^2\right) \frac{v_{cv}^2}{2} = \frac{\pi}{6} g \mu_r \rho_s d_{cd}^3, \qquad (5)$$

Rearranging Eq. (5), v_{cv} can be obtained as

$$v_{cv} = \sqrt{\frac{4}{3} \frac{g d_{cd}}{C_D} \frac{\rho_s}{\rho_g} \mu_r}, \qquad (6)$$

Eq. (6) describes the critical condition for the motion of the cutting particles. This condition means that the particles with smaller diameters than critical diameters are brought by air and the particles with bigger diameters than the critical diameters are broken again and again until their diameters become smaller than the particle's critical diameter. We discuss the motion of the particles having diameters not bigger than the critical diameters of the particles. According to Newton's second law, the motion for the flow of entraining cutting is given by

$$m_s \frac{dv_s}{dt} = F_d - f_r, \tag{7}$$

Substituting Eqs. (2)–(4) in Eq.(7).

$$m_s \frac{dv_s}{dt} = C_D A_r \rho_g \frac{(v_g - v_s)^2}{2} - \mu_r m_s g, \tag{8}$$

We assume that the end of the borehole is big enough. The particle is accelerated by giving the aerodynamical drag force. At last, the particle shows suspension movement with a high velocity. Let the aerodynamical drag coefficient is C_D' and the particle's suspension velocity is v_{sv}, then the result is

$$C_D' A_r \rho_g \cdot \frac{v_{sv}^2}{2} = m_s g, \tag{9}$$

The drag coefficient depends on Reynolds number and follows Newton's law of resistance. The Reynolds numbers Re_r and Re_{sv} correspond to C_D and C_D' respectively, and the difference between their values is very small. Hence, according to Newton's law of resistance, C_D and C_D' is be written as

$$C_D = \frac{A_r}{Re_r^k}, \quad C_D' = \frac{A_r}{Re_{sv}^k}, \tag{10}$$

where $Re_r = \rho_g \frac{v_g - v_s}{\eta_g} d_{sv}$, $Re_{sv} = \rho_g \frac{v_{sv}}{\eta_g} d_{sv}$ and η_g is the air's coefficient of viscosity; k represents the exponent in Newton's law of resistance, whose value is in the range of 0 to 1.

$$\frac{C_D}{C_D'} = \left(\frac{Re_{sv}}{Re_r}\right)^k = \left(\frac{v_{sv}}{v_g - v_s}\right)^k, \tag{11}$$

From Eqs. (9) and (11), C_D is

$$C_D = 2\left(\frac{v_{sv}}{v_g - v_s}\right)^k \cdot m_s g / A_r \rho_g v_{sv}^2, \tag{12}$$

substituting Eq. (12) into Eq. (8), the particle's motion in radial direction is given as

$$\frac{dv_s}{dt} = g\left(\frac{v_g - v_s}{v_{sv}}\right)^{2-k} - \mu_r g, \tag{13}$$

The dimensionless variables and parameters that are used in Eq. (13) are given by

$$\varphi = \frac{v_s}{v_g}, \quad T = \frac{gt}{v_g}, \quad \beta = \frac{v_{sv}}{v_g}, \tag{14}$$

Therefore, Eq.(13) becomes

$$\frac{d\varphi}{dT} = \left(\frac{1 - \varphi}{\beta}\right)^{2-k} - \mu_r, \tag{15}$$

In drilling with reverse air circulation, the unit of diameter is in millimeter, so the value of k in Eq. (15) is 0, and Eq. (15) becomes

$$\frac{d\varphi}{dT} = \left(\frac{1 - \varphi}{\beta}\right)^{2} - \mu_r. \tag{16}$$

Eq. (16) represents the mathematical model of the particle's motion in the radial direction.

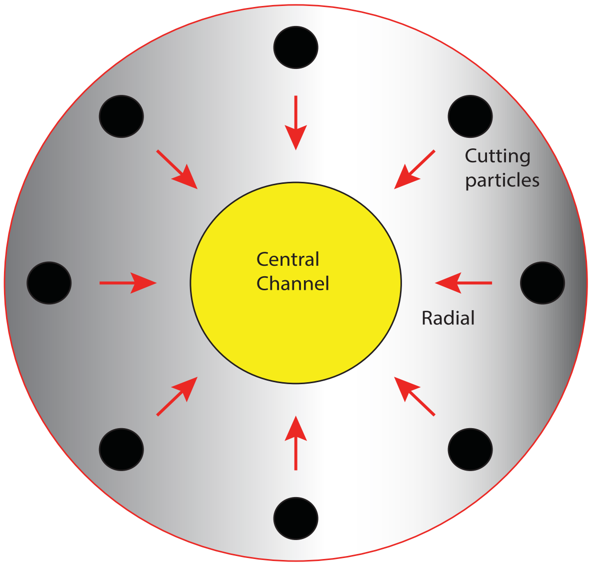

FIGURE 2. **Particle's motion in radial direction.**

IV. REFERENCE SOLUTIONS

The particles of the cutting rocks are static at the end of the borehole, hence the values of t and v_s are 0. Using initial condition, Eq. (16) is solved as given below [24]:

$$\frac{\beta}{2\sqrt{\mu_r}} \log\left|\frac{\frac{1}{\beta} - \sqrt{\mu_r}}{\frac{1}{\beta} + \sqrt{\mu_r}}\right| - \frac{\beta}{2\sqrt{\mu_r}} \log\left|\frac{\frac{1-\varphi}{\beta} - \sqrt{\mu_r}}{\frac{1-\varphi}{\beta} + \sqrt{\mu_r}}\right| = T. \tag{17}$$

V. THE ANN-BHCS APPROACH

In this paper, we have solved a problem that arises in the field of petroleum engineering. The mathematical model of the velocity of cutting particles in the radial direction during the process of reverse circulation of air in drilling is considered. An ANN based approach is developed and log-sigmoid is taken as activation function. The training of the weights is performed by a hybrid of biogeography based optimization and cuckoo search algorithm (BHCS). We have named our approach as ANN-BHCS algorithm.

A. CONSTRUCTION OF ANN MODEL

The general form of the approximate solution of ODEs of reverse circulation air drilling is considered in our research and the *nth* derivative of the solution is given as Eq.(18) [79]:

$$\hat{\varphi}(T) = \sum_{i=1}^{j} \alpha_i f\left(\omega_i T + \beta_i\right), \tag{18}$$

$$\frac{d^n}{dT^n}\hat{\varphi}(T) = \sum_{i=1}^{j} \alpha_i \frac{d^n}{dT^n} f\left(\omega_i T + \beta_i\right), \tag{19}$$

here α_i, ω_i and β_i are unknown weights whose values are real and are bounded, f is used for activation function and j is used for the number of neurons in our ANN model. Log-sigmoid is selected as an activation function for ANN

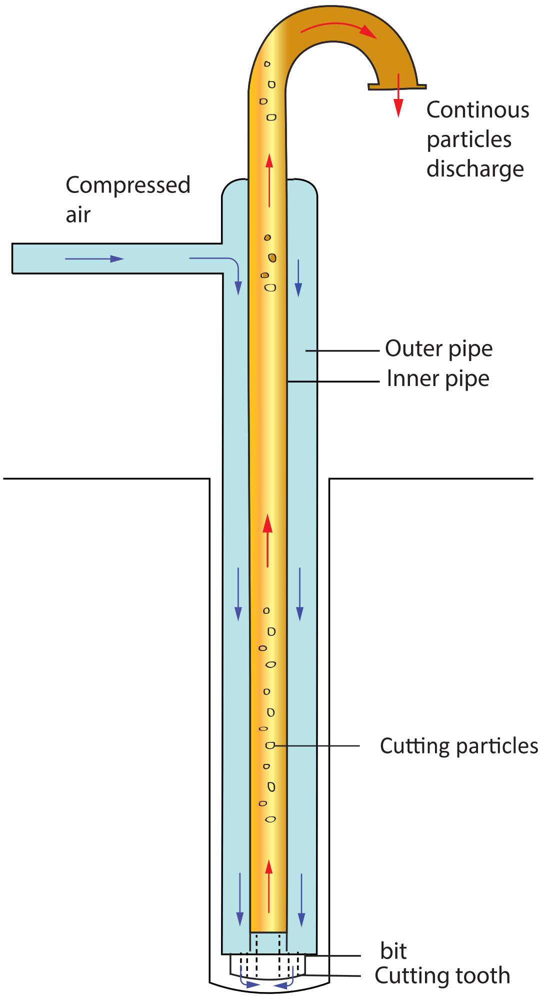

FIGURE 3. System of reverse air circulation drilling.

which is given as:

$$f(z) = \frac{1}{1+e^{-z}}, \tag{20}$$

Approximate solution and its first derivative for our proposed ANN model is given as:

$$\hat{\varphi}(T) = \sum_{i=1}^{j} \alpha_i \left(\frac{1}{1+e^{-(\omega_i T+\beta_i)}} \right), \tag{21}$$

$$\hat{\varphi}'(T) = \sum_{i=1}^{j} \alpha_i \omega_i \left(\frac{e^{-(\omega_i T+\beta_i)}}{\left(1+e^{-(\omega_i T+\beta_i)}\right)^2} \right). \tag{22}$$

B. OBJECTIVE FUNCTION

The fitness function for the problem is a sum of the mean squared errors E1 and E2 which is given as:

$$minimize \quad E = E_1 + E_2, \tag{23}$$

where E_1 is related to ODE and E_2 is related to the initial or boundary conditions. For Eq.(16), E_1 and E_2 are given as:

$$E_1 = \frac{1}{N+1} \sum_{m=0}^{N} \left(\frac{d\hat{\varphi}}{dT} - \left(\frac{1-\hat{\varphi}}{\beta} \right)^2 + \mu_r \right)^2, \tag{24}$$

$$E_2 = (\varphi_0(T) - 0)^2. \tag{25}$$

In Eqs.(21,22), α, ω and β are the weights that can be adjusted in order to minimize E_1 and E_2 such that E approaches to 0. Hence, the approximate solution $\hat{\varphi}$ of the problem will be near to the exact solution φ.

C. CUCKOO SEARCH

Inspired by the cuckoo bird's breeding behavior, a meta-heuristic algorithm was developed which is called the cuckoo search algorithm [80]. The female bird lays eggs in the nests of other birds and they unintentionally raise her brood. When the host bird finds the cuckoo's egg in the nest, it either starts making her brood elsewhere or throw the egg out of her nest [81].

In the cuckoo search algorithm, the egg of the host bird shows a solution, and the egg of the cuckoo bird shows a new candidate solution. The CS algorithm works according to the three rules that are as follows [82]: (1) at a time, every cuckoo bird lays only one egg and put it in the host's nest; (2) those nests which have eggs of high quality which are better solutions will go to the next generation, and (3) the number of hosts' nests is fixed, and the host bird can find an alien egg with certain probability.

Assuming $\boldsymbol{x_i} = (x_{i1}, x_{i2}, \cdots, x_{iD})$ as the position for the *ith* egg (solution) then updated solution $x_i{}^{new}$ is generated by Levy flights as given below:

$$\begin{aligned} x_i^{new} &= x_i^{old} + \alpha \left(x_l - x_g\right) \oplus \text{Levy}(\beta), \\ &= x_i^{old} + \frac{0.01u}{|v|^{1/\beta}} \left(x_i - x_g\right), \end{aligned} \tag{26}$$

where the product $\bigoplus$ is entry-wise multiplication; the Levy flight exponent is denoted by β; the step size for a cuckoo is determined by a positive parameter α; the best solutions in the current population are denoted by x_g; u and v are used for random numbers:

$$u \sim N\left(0, \sigma_u^2\right), \quad v \sim N\left(0, \sigma_v^2\right), \tag{27}$$

$$\sigma_u = \left[\frac{\sin(\pi\beta/2) \cdot \Gamma(1+\beta)}{2^{(\beta-1)/2}\beta \cdot \Gamma\left(\frac{1+\beta}{2}\right)} \right]^{1/\beta}, \quad \sigma_v = 1, \tag{28}$$

where Γ is used for Gamma function, and β controls the value of σ_u. There is a discovery operator in CS which is used to replace the discovered nests according to the probability pa. To update the solution, the following equation is used:

$$x_{ij}^{new} = \begin{cases} x_{ij}^{\text{old}} + \text{rand} \cdot \left(x_{r1,j}(k) - x_{r2\,j}(k)\right) & \text{if } P > pa, \\ x_{ij}^{\text{old}}(k) & \text{else}, \end{cases} \tag{29}$$

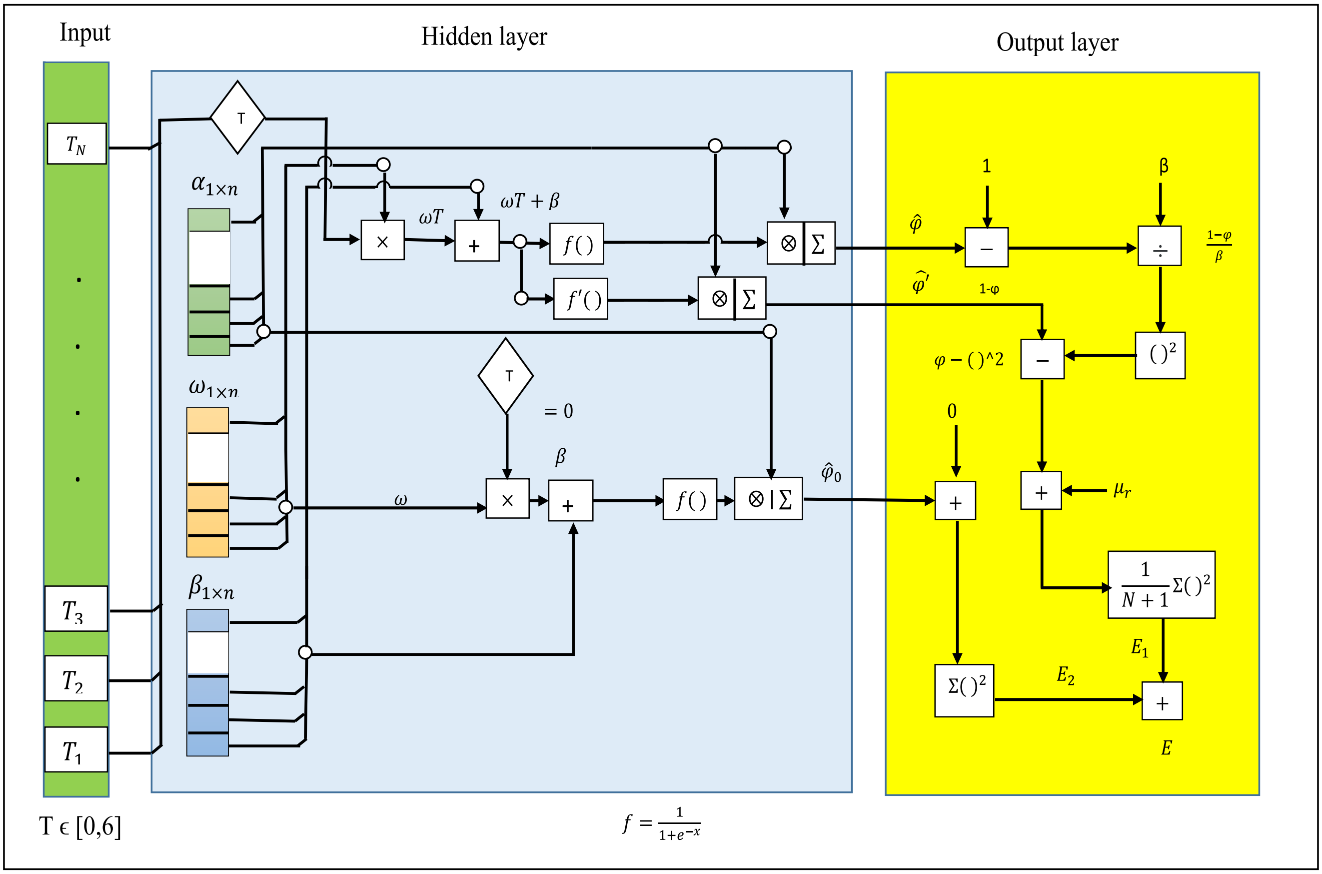

FIGURE 4. ANN structure for the problem.

where x_{ij}^{new} is the jth element of the ith solution x_i^{new};$x_{r1,j}$ and $x_{r2,j}$ are the jth elements of the two solutions x_{r1} and x_{r2}, where $r1$ and $r2$ are two different integers in the interval $[1, NP]$, where NP represents the population size, discovery probability is denoted by pa, P and rand are some random numbers belong to the interval [0, 1].

D. BIOGEOGRAPHY-BASED OPTIMIZATION

Biogeography based optimization (BBO) is an evolutionary algorithm that is inspired by different characteristics of species living in the islands [83]. In BBO, each habitat is considered as a candidate solution having some habitat's suitability index (HSI), which is employed for the measurement of the quality of a habitat. A habitat (solution) is represented by some suitability index variables (SIV). Two types of operators are used in BBO, migration, and mutation that are employed for the evolution of the population. In the migration process, the solutions with high HSI share their features with the solutions having low HSI and the solutions with low HSI accept new features from the solutions with high HSI.

In BBO, the population is randomly initialized with NP habitats (solutions). Each generation sorts the population from the best to the worst and each habitat is assigned with immigration and emigration rates λ and μ respectively:

$$\begin{cases} \lambda_i = I\left(1 - \dfrac{S_i}{NP}\right), \\ \mu_i = E\dfrac{S_i}{NP}. \end{cases} \tag{30}$$

here I and E are used for immigration and emigration rates respectively where I = E = 1; S_i represents the number of species in population and $S_i = NP - i$. Accordingly, for the best solution, the S_i value is $NP - 1$ and for the second best solution the S_i value is $NP - 2$ and for the worst solution, the S_i value is 0. The migration mixes the features within the population that modifies the solutions. After migration, to modify the solutions, BBO also uses the mutation operator.

E. BBO BASED HETEROGENEOUS CUCKOO SEARCH ALGORITHM

CS and BBO are hybridized because CS uses the Levy flights to modify the solution which is good at exploration and BBO employs the migration operator to modify the solution which is good at exploitation. Combining the exploration and exploitation, a hybrid metaheuristic is developed which is known as BBO based heterogeneous cuckoo search (BHCS)

TABLE 2. Solutions obtained for case 1.

T	Analytical [24]	ANN-BHCS	GA	PSO	Bat algorithm	MVO
0	0.0000000	0.0005401	-0.0159016	-0.0000272	0.0011159	0.0155949
0.2	0.8177000	0.8204161	0.8940101	0.8639582	0.6839090	0.9213168
0.4	0.8815076	0.8817631	0.8965692	0.8934084	0.8778198	0.9117998
0.6	0.8997209	0.9000188	0.8965855	0.9040057	0.9023474	0.9106027
0.8	0.9062801	0.9064060	0.8965934	0.9079638	0.9053755	0.9106000
1	0.9088330	0.9088077	0.8966008	0.9096068	0.9059199	0.9106000
1.2	0.9098563	0.9097774	0.8966077	0.9101647	0.9104845	0.9106000
1.4	0.9102714	0.9101944	0.8966142	0.9103558	0.9106989	0.9106000
1.6	0.9104405	0.9103831	0.8966203	0.9104247	0.9106999	0.9106000
1.8	0.9105096	0.9104717	0.8966259	0.9104493	0.9107000	0.9106000
2	0.9105378	0.9105145	0.8966312	0.9104577	0.9107000	0.9106000
2.2	0.9105493	0.9105356	0.8966362	0.9104602	0.9107000	0.9106000
2.4	0.9105540	0.9105461	0.8966409	0.9104605	0.9107000	0.9106000
2.6	0.9105559	0.9105514	0.8966452	0.9104600	0.9107000	0.9106000
2.8	0.9105567	0.9105540	0.8966493	0.9104592	0.9107000	0.9106000
3	0.9105571	0.9105553	0.8966531	0.9104583	0.9107000	0.9106000
3.2	0.9105572	0.9105560	0.8966567	0.9104573	0.9107000	0.9106000
3.4	0.9105572	0.9105563	0.8966600	0.9104563	0.9107000	0.9106000
3.6	0.9105573	0.9105565	0.8966631	0.9104553	0.9107000	0.9106000
3.8	0.9105573	0.9105565	0.8966661	0.9104542	0.9107000	0.9106000
4	0.9105573	0.9105566	0.8966688	0.9104531	0.9107000	0.9106000
4.2	0.9105573	0.9105566	0.8966714	0.9104520	0.9107000	0.9106000
4.4	0.9105573	0.9105566	0.8966738	0.9104508	0.9107000	0.9106000
4.6	0.9105573	0.9105566	0.8966760	0.9104496	0.9107000	0.9106000
4.8	0.9105573	0.9105566	0.8966782	0.9104484	0.9107000	0.9106000
5	0.9105573	0.9105566	0.8966801	0.9104472	0.9107000	0.9106000
5.2	0.9105573	0.9105566	0.8966820	0.9104459	0.9107000	0.9106000
5.4	0.9105573	0.9105566	0.8966837	0.9104446	0.9107000	0.9106000
5.6	0.9105573	0.9105566	0.8966853	0.9104432	0.9107000	0.9106000
5.8	0.9105573	0.9105566	0.8966868	0.9104419	0.9107000	0.9106000
6	0.9105573	0.9105566	0.8966883	0.9104405	0.9107000	0.9106000

algorithm. The proposed BHCS algorithm has two main steps that are heterogeneous cuckoo search and biogeography based discovery. The two steps are explained in the next sections.

1) STRATEGY OF HETEROGENEOUS CUCKOO SEARCH

In first step, BHCS uses the Levy flights and quantum mechanism based heterogeneous cuckoo search. This strategy is inspired by quantum mechanism and was first presented in [81], [84]. The rules to update the solutions by the heterogeneous cuckoo search are given as follows [81], [84]:

$$x_i^{new} = \begin{cases} x_i^{old} + \alpha \cdot \left(x_i - x_g\right) \oplus \text{Levy}(\beta) & \frac{2}{3} < sr \leqslant 1(a), \\ \bar{x} + L \cdot \left(\bar{x} - x_i^{old}\right) & \frac{1}{3} < sr \leqslant \frac{2}{3}(b). \\ x_i^{old} + \varepsilon \cdot \left(x_g - x_i^{old}\right) & \text{else } (c)\,. \end{cases} \tag{31}$$

where $L = \delta \ln(1/\eta)$, $\varepsilon = \delta \exp(\eta)$, x_g is used for solution that is best at current iteration; $\bar{x} = \frac{1}{NP}\sum_{i=1}^{NP} x_i$ represents the mean of the solutions; sr and η are randomly selected numbers belong to the interval [0, 1]. Eq.(31) shows that heterogeneous cuckoo search employs three equations to update the solutions with the same probabilities. The first equation is based on Levy flights in original CS and the second and third equations to update the solutions are based on quantum mechanism. Updating the solutions using heterogeneous rules diversify the search space and follows the direction towards the real global region.

2) BIOGEOGRAPHY-BASED DISCOVERY OPERATOR

In the second step, New solutions are generated using a discovery operator. When the host bird finds an alien egg with probability pa, it abandons the old nest and makes a new nest on the basis of the migration operator. Initially, solutions are sorted from best to worst, then an immigration rate μ is assigned to each solution:

$$\mu_l = E\frac{S_i}{NP}. \tag{32}$$

where E represents the emigration rate having maximum value of 1; $S_i = NP - i$ represents the number of species in solutions. In biogeography based discovery operator, the solutions having best fitness share their characteristics with other solutions which help to enhance the exploitation.

F. OVERALL BHCS ALGORITHM

The BHCS algorithm uses a cascading structure for the implementation of its two search steps. The coordination between the search strategies of the heterogeneous cuckoo search and biogeography based discovery operator can efficiently balance the exploitation and exploration.

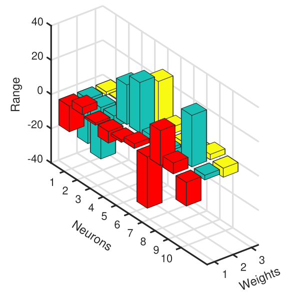

(a) Weights obtained by ANN-BHCS algorithm.

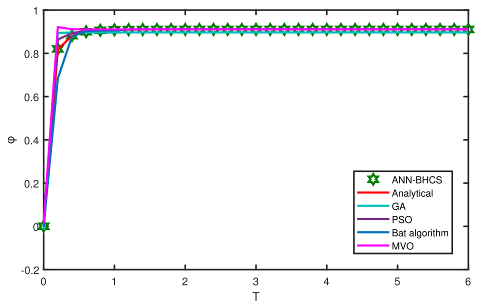

(b) Solutions obtained by ANN-BHCS algorithm and other algorithms.

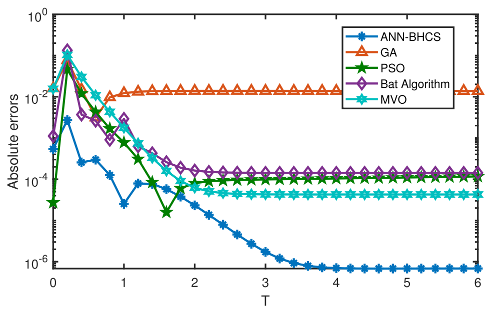

(c) Absolute errors obtained by ANN-BHCS algorithm and other algorithms.

FIGURE 5. Results obtained for case 1.

VI. RESULTS AND DISCUSSION

In this paper, we have implemented the ANN-BHCS algorithm for the solution of the ODEs that model the motion of particles in the radial direction during the drilling process with the reverse circulation of air. The motion of the cutting particles in the radial direction is discussed. The solutions obtained by Zhu *et al.* [24] are considered as reference solutions. To compare the results of the ANN-BHCS algorithm, we have solved the problem by genetic algorithm (GA), particle swarm optimization (PSO), bat algorithm and multiverse optimizer (MVO).

Four statistical operators are employed to test the efficiency of the designed algorithm. These operators are MAD, TIC and ENSE. Mathematical forms of these operators are given

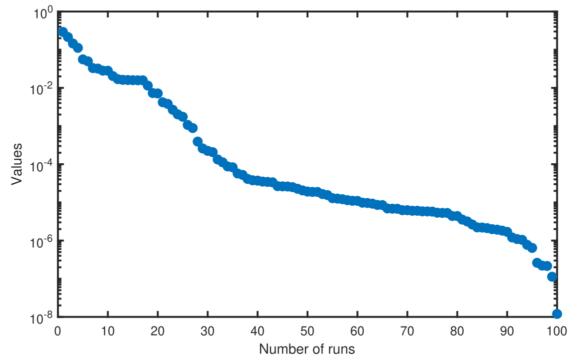

(a) Convergence of the fitness values.

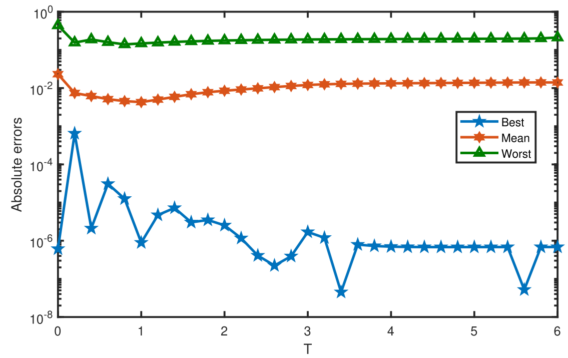

(b) Best, mean and worst values of errors.

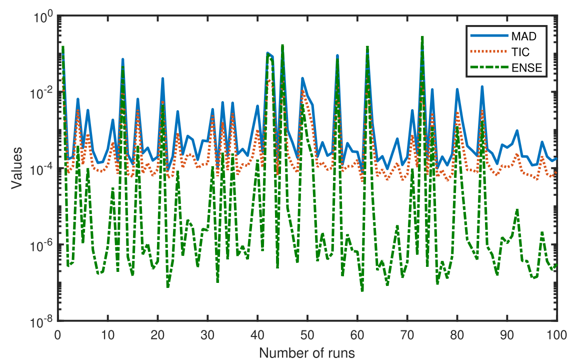

(c) Values of performance metrics.

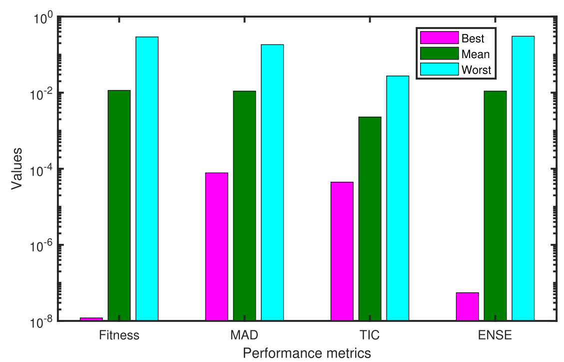

(d) Minimum, mean and maximum values of performance metrics.

FIGURE 6. Performance analysis of ANN-BHCS algorithm for case 1.

as follows:

$$MAD = \frac{1}{n}\sum_{i=1}^{n}\left|\varphi_i - \hat{\varphi}_i\right|, \tag{33}$$

$$TIC = \frac{\sqrt{\frac{1}{n}\sum_{i=1}^{n}\left(\varphi_i - \hat{\varphi}_i\right)^2}}{\left(\sqrt{\frac{1}{n}\sum_{i=1}^{n}\varphi_i^2} + \sqrt{\frac{1}{n}\sum_{i=1}^{n}\hat{\varphi}_i^2}\right)}, \tag{34}$$

$$NSE = 1 - \frac{\sum_{i=1}^{n}\left(\varphi_i - \hat{\varphi}_i\right)^2}{\sum_{i=1}^{n}\left(\varphi_i - \bar{\varphi}_i\right)^2}, \quad \bar{\varphi}_i = \frac{1}{n}\sum_{i=1}^{n}\varphi_i, \tag{35}$$

$$ENSE = 1 - NSE. \tag{36}$$

here n denotes the number of grid points in approximate solution.

A. PARTICLE'S VELOCITY IN RADIAL DIRECTION

In the model of the radial velocity of the particles, we have considered five cases on the basis of the values of μ_r and β. The initial condition imposed on these cases is $\varphi(0) = 0$ because at the bottom of the borehole, the particles are at rest and their velocity is 0.

Each hidden layer in the ANN architecture has 10 neurons with 30 unknown weights. The step size is taken as h = 0.2, and there are 31 grid points in the entire domain that is [0,6]. We have simulated the ANN-BHCS algorithm with 100 runs to assess the reliability and convergence of our approach.

1) CASE 1

In this case, the values of $\mu_r = 0.2$ and $\beta = 0.2$. Using the values, Eq.(16) becomes:

$$\frac{d\varphi}{dT} = \left(\frac{1-\varphi}{0.2}\right)^2 - 0.2, \tag{37}$$

using Eq.(37), the minimization objective function for this case is given by:

$$E = \frac{1}{31}\sum_{m=0}^{N}\left(\frac{d\hat{\varphi}}{dT} - \left(\frac{1-\hat{\varphi}}{0.2}\right)^2 + 0.2\right)^2 + (\varphi(0) - 0)^2. \tag{38}$$

We have taken ten neurons in our ANN model. The approximate solutions obtained using the ANN-BHCS algorithm contains 10 terms, one neuron corresponds to one term of solution. Convergence of the fitness values for 100 runs is given in Figure(6a).

The minimum fitness value obtained for this case is $1.1977E-08$. Weights obtained by the ANN-BHCS algorithm to minimize the fitness function are plotted in Figure(5a). Using these weights, the series solution for case 1 is given as follows:

$$\begin{aligned}\hat{\varphi}(T) = &\frac{-14.9725711437890}{1+e^{-(-26.0115480832910*T-1.84268363995668)}} \\ &+ \frac{4.24755258262079}{1+e^{-(-29.9999959386755*T-0.452220232464229)}} \\ &+ \frac{-1.22273335804037}{1+e^{-(-6.55087234613671*T-1.84441540808597)}} \\ &+ \frac{-6.76729788945139}{1+e^{-(23.0887477954241*T+17.4464254308947)}} \\ &+ \frac{-1.36613361868158}{1+e^{-(29.3894332403492*T+25.8507385755634)}} \\ &+ \frac{2.67623305581058}{1+e^{-(2.81898188149628*T+3.94697322620978)}} \\ &+ \frac{-29.9315404441912}{1+e^{-(-4.43709353698262*T-6.22247514806738)}} \\ &+ \frac{20.3113349283508}{1+e^{-(-2.71944275677821*T-5.24984964481302)}} \\ &+ \frac{6.36775504863650}{1+e^{-(29.9998541142396*T+3.10695945223067)}} \\ &+ \frac{-13.8181857402193}{1+e^{-(-2.71408030194718*T-5.26890221647680)}}.\end{aligned} \tag{39}$$

TABLE 3. Comparison of absolute errors of ANN-BHCS algorithm and other algorithms for case 1.

T	ANN-BHCS	GA	PSO	Bat algorithm	MVO
0	5.4012E-04	1.5902E-02	2.7154E-05	1.1159E-03	1.5595E-02
0.2	2.7161E-03	7.6310E-02	4.6258E-02	1.3379E-01	1.0362E-01
0.4	2.5551E-04	1.5062E-02	1.1901E-02	3.6878E-03	3.0292E-02
0.6	2.9796E-04	3.1354E-03	4.2848E-03	2.6265E-03	1.0882E-02
0.8	1.2589E-04	9.6867E-03	1.6837E-03	9.0464E-04	4.3199E-03
1	2.5267E-05	1.2232E-02	7.7378E-04	2.9131E-03	1.7670E-03
1.2	7.8899E-05	1.3249E-02	3.0844E-04	6.2819E-04	7.4370E-04
1.4	7.6948E-05	1.3657E-02	8.4391E-05	4.2745E-04	3.2860E-04
1.6	5.7434E-05	1.3820E-02	1.5780E-05	2.5940E-04	1.5950E-04
1.8	3.7828E-05	1.3884E-02	6.0307E-05	1.9039E-04	9.0400E-05
2	2.3222E-05	1.3907E-02	8.0108E-05	1.6220E-04	6.2200E-05
2.2	1.3683E-05	1.3913E-02	8.9119E-05	1.5070E-04	5.0700E-05
2.4	7.9041E-06	1.3913E-02	9.3498E-05	1.4600E-04	4.6000E-05
2.6	4.5726E-06	1.3911E-02	9.5882E-05	1.4410E-04	4.4100E-05
2.8	2.7204E-06	1.3907E-02	9.7475E-05	1.4330E-04	4.3300E-05
3	1.7204E-06	1.3904E-02	9.8794E-05	1.4290E-04	4.2900E-05
3.2	1.1946E-06	1.3901E-02	9.9875E-05	1.4280E-04	4.2800E-05
3.4	9.2542E-07	1.3897E-02	1.0089E-04	1.4280E-04	4.2800E-05
3.6	7.9163E-07	1.3894E-02	1.0204E-04	1.4270E-04	4.2700E-05
3.8	7.2756E-07	1.3891E-02	1.0312E-04	1.4270E-04	4.2700E-05
4	6.9842E-07	1.3888E-02	1.0422E-04	1.4270E-04	4.2700E-05
4.2	6.8622E-07	1.3886E-02	1.0535E-04	1.4270E-04	4.2700E-05
4.4	6.8186E-07	1.3884E-02	1.0650E-04	1.4270E-04	4.2700E-05
4.6	6.8091E-07	1.3881E-02	1.0769E-04	1.4270E-04	4.2700E-05
4.8	6.8125E-07	1.3879E-02	1.0890E-04	1.4270E-04	4.2700E-05
5	6.8197E-07	1.3877E-02	1.1014E-04	1.4270E-04	4.2700E-05
5.2	6.8268E-07	1.3875E-02	1.1141E-04	1.4270E-04	4.2700E-05
5.4	6.8326E-07	1.3874E-02	1.1272E-04	1.4270E-04	4.2700E-05
5.6	6.8369E-07	1.3872E-02	1.1405E-04	1.4270E-04	4.2700E-05
5.8	6.8399E-07	1.3870E-02	1.1542E-04	1.4270E-04	4.2700E-05
6	6.8420E-07	1.3869E-02	1.1682E-04	1.4270E-04	4.2700E-05

Numerical solutions obtained by the ANN-BHCS algorithm and other algorithms are presented in Table (2). The graphs of numerical solutions are plotted in Figure (5b). The comparison of absolute errors of ANN-BHCS and other algorithms is presented in Table (3) and Figure (5c). From Table (3) and Figure (5c), we can see that the ANN-BHCS algorithm given better results than other algorithms.

Statistical analysis of absolute errors of ANN-BHCS algorithm is presented in Table (6) and Figure (6b). The minimum and mean values of absolute errors are in the range $E-04$ to $E-08$, and $E-02$ to $E-03$ respectively, which shows the accuracy of the ANN-BHCS algorithm. Values of performance metrics for 100 runs are plotted in Figure (6c). The values of performance metrics in terms of best, mean and worst are shown in Table (4) and are also given in Figure (6d).

TABLE 4. Analysis of the values of fitness function and performance metrics obtained by ANN-BHCS algorithm for case 1.

Metrics	Best	Mean	Worst
Fitness	1.2974E-08	1.1200E-02	2.8450E-01
MAD	7.8026E-05	1.1000E-02	1.8330E-01
TIC	4.4484E-05	2.3000E-03	2.7500E-02
ENSE	5.5261E-08	1.1000E-02	3.0510E-01

TABLE 5. Convergence analysis of performance metrics for case 1.

Metrics	≤E-03	≤E-04	≤E-05	≤E-06
Fitness	83	76	70	47
MAD	87	72	4	0
TIC	91	79	42	0
ENSE	92	87	79	73

The minimum values of the fitness function, MAD, TIC and ENSE are $1.2974E-08$, $7.8026E-05$, $4.4484E-05$ and $5.5261E-08$ respectively, which shows that the solutions obtained by the ANN-BHCS algorithm are very close to the analytical solution.

Convergence analysis of performance metrics for case 1 is given in Table (5). Histograms and box-plots for performance metrics and fitness function are given in Figure (7). Histogram and box plots of the fitness values show that most of the values are close to zero. The box-plots of the fitness values show that 50% of the values are in the interquartile range which is $E-03$ to $E-06$ and 25% of the values are less than $E-06$.

Histogram and box plots of MAD values show that more than 80% of the values are less than or equal to $E-03$. The box plot of MAD values shows that more than 75% of the values are in the range $E-02$ to $E-06$. Similarly, the histogram of TIC values shows that more than 90% of the values are less than or equal to $E-03$ and the box plot of the TIC values shows that more than 75% of the values are in the range $E-03$ to $E-06$.

Histogram of the ENSE values shows that more than 90% of the values are less than or equal to $E-03$ and box plot shows that 75% of the values are in the range $E-05$ to $E-08$. The above discussion justifies the efficiency of the ANN-BHCS algorithm for the solution of ODEs.

2) CASE 2

In this case, the values of $\mu_r = 0.2$ and $\beta = 0.6$. Using these values, Eq.(16) becomes

$$\frac{d\varphi}{dT} = \left(\frac{1-\varphi}{0.6}\right)^2 - 0.2, \tag{40}$$

using Eq.(40), the minimization objective function for this case can be written as:

$$E = \frac{1}{31}\sum_{m=0}^{N}\left(\frac{d\hat{\varphi}}{dT} - \left(\frac{1-\hat{\varphi}}{0.6}\right)^2 + 0.2\right)^2 + (\varphi(0)-0)^2. \tag{41}$$

TABLE 6. Statistical analysis of absolute errors in ANN-BHCS algorithm solutions for case 1.

T	Min	Mean	SD
0	6.1108E-07	2.3133E-02	7.1035E-02
0.2	6.4788E-04	7.4198E-03	2.0521E-02
0.4	2.1095E-06	6.1725E-03	2.2922E-02
0.6	3.0932E-05	5.1318E-03	2.0665E-02
0.8	1.2568E-05	4.5565E-03	1.8008E-02
1	8.9092E-07	4.2892E-03	1.7326E-02
1.2	4.7104E-06	4.9967E-03	1.9063E-02
1.4	7.2304E-06	5.8875E-03	2.2523E-02
1.6	3.0368E-06	6.9037E-03	2.6551E-02
1.8	3.4899E-06	7.7966E-03	3.0043E-02
2	2.5327E-06	8.5184E-03	3.2604E-02
2.2	1.1632E-06	9.1746E-03	3.4408E-02
2.4	4.0836E-07	9.8520E-03	3.5884E-02
2.6	2.2324E-07	1.0619E-02	3.7501E-02
2.8	3.9214E-07	1.1358E-02	3.9132E-02
3	1.6932E-06	1.2062E-02	4.0845E-02
3.2	1.1946E-06	1.2573E-02	4.2251E-02
3.4	4.4889E-08	1.2885E-02	4.3160E-02
3.6	7.9163E-07	1.3075E-02	4.3689E-02
3.8	7.2756E-07	1.3204E-02	4.4024E-02
4	6.9842E-07	1.3310E-02	4.4285E-02
4.2	6.8622E-07	1.3404E-02	4.4532E-02
4.4	6.8186E-07	1.3494E-02	4.4788E-02
4.6	6.8091E-07	1.3587E-02	4.5060E-02
4.8	6.8125E-07	1.3679E-02	4.5353E-02
5	6.8197E-07	1.3768E-02	4.5661E-02
5.2	6.8268E-07	1.3865E-02	4.5974E-02
5.4	6.8326E-07	1.3963E-02	4.6271E-02
5.6	5.1958E-08	1.4039E-02	4.6517E-02
5.8	6.8399E-07	1.4069E-02	4.6645E-02
6	6.8420E-07	1.4025E-02	4.6551E-02

The fitness value obtained for this case is $4.2369E-10$. Convergence of the fitness values for 100 runs is given in Figure(9a). Weights obtained to minimize the fitness function are given in Figure(8a). Using these weights, the series solution for this case is given as:

$$\begin{aligned}
\hat{\varphi}(T) = {} & \frac{-2.56333854675081}{1+e^{-(-14.9737951773003*T-4.49440776545225)}} \\
& + \frac{4.38914557642178}{1+e^{-(-13.4852437480416*T-5.97717662826386)}} \\
& + \frac{8.17052649405911}{1+e^{-(-5.21681521102496*T-7.68199890138727)}} \\
& + \frac{-1.60908958149487}{1+e^{-(-0.993426318916703*T-6.33657960595496)}} \\
& + \frac{-0.0932430207253772}{1+e^{-(8.39209185800148*T+3.97217607383839)}} \\
& + \frac{-2.03356385047608}{1+e^{-(-3.07804622968367*T-1.87188416380365)}} \\
& + \frac{-6.02624978872788}{1+e^{-(-5.16561956740399*T-4.08658080324857)}} \\
& + \frac{0.824922427843496}{1+e^{-(1.50749589298907*T+0.965526067515892)}} \\
& + \frac{2.74381813431155}{1+e^{-(-9.39842562762194*T-6.03941180706777)}}
\end{aligned}$$

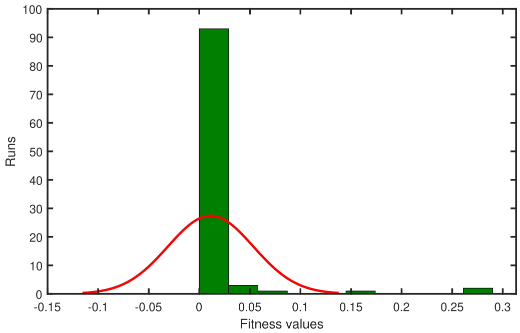

(a) Histogram for fitness values.

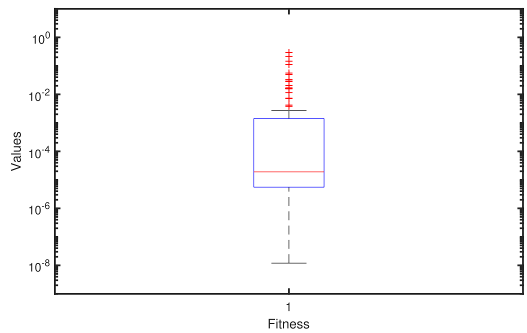

(b) Box plot for fitness values.

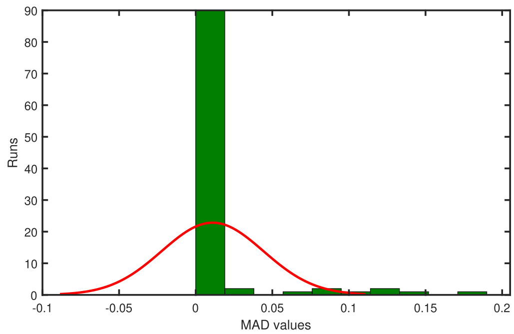

(c) Histogram for MAD values.

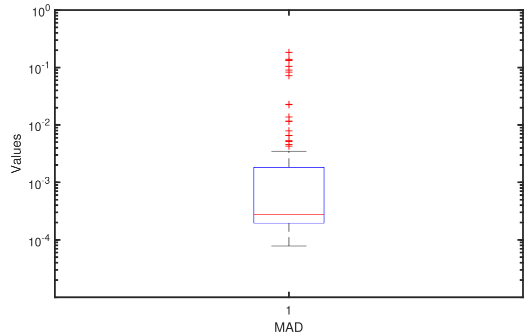

(d) Box plot for MAD values.

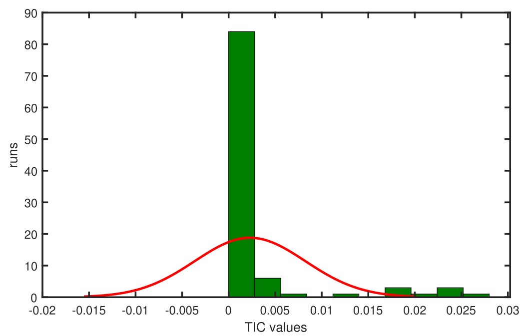

(e) Histogram for TIC values.

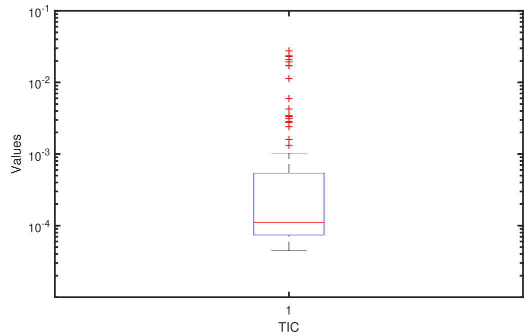

(f) Box plot for TIC values.

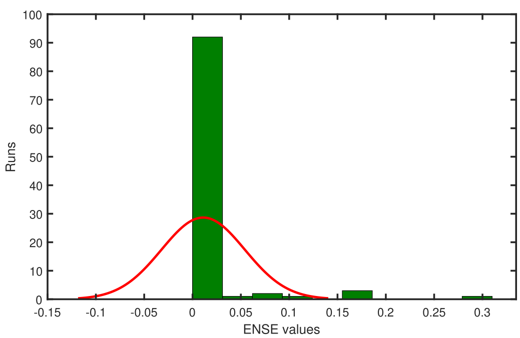

(g) Histogram for ENSE values.

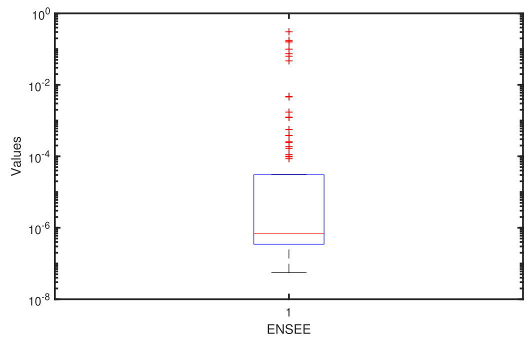

(h) Box plot for ENSE values.

FIGURE 7. Histograms and box plots of values of performance metrics for case 1.

TABLE 7. Solutions obtained for case 2.

T	Analytical [24]	ANN-BHCS	GA	PSO	Bat algorithm	MVO
0	0.00000000	-0.00000092	0.03707610	-0.00003472	-0.00047490	0.00249917
0.2	0.32986013	0.32985918	0.38951923	0.32242913	-0.24328309	0.30665001
0.4	0.48170008	0.48170864	0.52871828	0.47916684	2.86213724	0.48519697
0.6	0.56603430	0.56602544	0.58626226	0.56428393	0.69305898	0.60339735
0.8	0.61779744	0.61778985	0.69589812	0.61590769	0.82019169	0.66542830
1	0.65153839	0.65154132	0.72258641	0.65020387	0.78070646	0.69305002
1.2	0.67440177	0.67441125	0.72520735	0.67402053	0.75266380	0.70440054
1.4	0.69030435	0.69031486	0.72604042	0.69068867	0.74181597	0.70890826
1.6	0.70156732	0.70157581	0.72633437	0.70224742	0.73806460	0.71067418
1.8	0.70964692	0.70965241	0.72643845	0.71017110	0.73681164	0.71136233
2	0.71549619	0.71549873	0.72647530	0.71560085	0.73639926	0.71162994
2.2	0.71975891	0.71975891	0.72648835	0.71947750	0.73626463	0.71173394
2.4	0.72288043	0.72287834	0.72649297	0.72263495	0.73622091	0.71177434
2.6	0.72517434	0.72517062	0.72649461	0.72554321	0.73620677	0.71179003
2.8	0.72686443	0.72685952	0.72649519	0.72785430	0.73620222	0.71179613
3	0.72811202	0.72810634	0.72649539	0.72923169	0.73620076	0.71179850
3.2	0.72903427	0.72902819	0.72649546	0.72994571	0.73620031	0.71179942
3.4	0.72971672	0.72971060	0.72649549	0.73032406	0.73620018	0.71179977
3.6	0.73022212	0.73021624	0.72649550	0.73053959	0.73620015	0.71179991
3.8	0.73059662	0.73059122	0.72649550	0.73066995	0.73620017	0.71179997
4	0.73087423	0.73086951	0.72649550	0.73075177	0.73620020	0.71179999
4.2	0.73108008	0.73107618	0.72649550	0.73080421	0.73620025	0.71180000
4.4	0.73123277	0.73122975	0.72649550	0.73083826	0.73620031	0.71180000
4.6	0.73134603	0.73134395	0.72649550	0.73086066	0.73620039	0.71180000
4.8	0.73143006	0.73142893	0.72649550	0.73087570	0.73620048	0.71180000
5	0.73149242	0.73149220	0.72649550	0.73088623	0.73620060	0.71180000
5.2	0.73153869	0.73153935	0.72649550	0.73089424	0.73620075	0.71180000
5.4	0.73157302	0.73157450	0.72649550	0.73090125	0.73620093	0.71180000
5.6	0.73159850	0.73160074	0.72649550	0.73090861	0.73620116	0.71180000
5.8	0.73161741	0.73162034	0.72649550	0.73091775	0.73620144	0.71180000
6	0.73163144	0.73163500	0.72649550	0.73093048	0.73620179	0.71180000

$$+\frac{-4.88366839334966}{1+e^{-(-7.54672211951740*T-3.63556335983704)}}. \tag{42}$$

Numerical solutions obtained for this case are given in Table (7). The solutions are also plotted in Figure (8b), which shows that the solution obtained by the ANN-BHCS algorithm is very close to the solution obtained by [24].

The accuracy of the solution obtained by the ANN-BHCS algorithm is also clear from the comparison of absolute errors in Table (8) and Figure (8c). Statistical analysis for absolute errors is given in Table (11) and minimum, mean, and maximum values of absolute errors are also plotted in Figure (9b). The minimum values of absolute errors are in the range $E-06$ to $E-09$, mean values are in the range $E-03$ to $E-04$, and the standard deviation in absolute errors at all points of the domain is about $E-03$.

Figure (9c) shows the values of performance metrics and fitness function. Table (9) and Figure (9d) illustrate the values of performance metrics in terms of best, mean, and worst. Convergence analysis of performance metrics for 100 runs is given in Table (10).

Histograms and box plots of performance metrics and fitness function are given in Figure (10). Histogram of the fitness values shows that 100% of the values are less than or equal to $E-03$ and box plot of the fitness values shows that more than 75% of the values are between $E-06$ and $E-10$. Histogram of the MAD values shows that more than 95% of the values are less than or equal to $E-03$ and the box plot shows that more than 75% of the values are in the range $E-03$ to $E-06$. Histogram of the TIC values shows that 100% of the values are less than or equal to $E-03$ and box plot shows that more than 75% of the values are in the range $E-04$ to $E-06$.

TABLE 8. Comparison of absolute errors of ANN-BHCS algorithm and other algorithms for case 2.

T	ANN-BHCS	GA	PSO	Bat algorithm	MVO
0	9.1670E-07	3.7076E-02	3.4720E-05	4.7490E-04	2.4992E-03
0.2	9.5405E-07	5.9659E-02	7.4310E-03	5.7314E-01	2.3210E-02
0.4	8.5627E-06	4.7018E-02	2.5332E-03	2.3804E+00	3.4969E-03
0.6	8.8599E-06	2.0228E-02	1.7504E-03	1.2702E-01	3.7363E-02
0.8	7.5824E-06	7.8101E-02	1.8897E-03	2.0239E-01	4.7631E-02
1	2.9299E-06	7.1048E-02	1.3345E-03	1.2917E-01	4.1512E-02
1.2	9.4841E-06	5.0806E-02	3.8124E-04	7.8262E-02	2.9999E-02
1.4	1.0518E-05	3.5736E-02	3.8433E-04	5.1512E-02	1.8604E-02
1.6	8.4927E-06	2.4767E-02	6.8010E-04	3.6497E-02	9.1069E-03
1.8	5.4953E-06	1.6792E-02	5.2418E-04	2.7165E-02	1.7154E-03
2	2.5460E-06	1.0979E-02	1.0466E-04	2.0903E-02	3.8662E-03
2.2	5.7879E-09	6.7294E-03	2.8141E-04	1.6506E-02	8.0250E-03
2.4	2.0895E-06	3.6125E-03	2.4548E-04	1.3340E-02	1.1106E-02
2.6	3.7153E-06	1.3203E-03	3.6887E-04	1.1032E-02	1.3384E-02
2.8	4.9055E-06	3.6924E-04	9.8987E-04	9.3378E-03	1.5068E-02
3	5.6838E-06	1.6166E-03	1.1197E-03	8.0887E-03	1.6314E-02
3.2	6.0790E-06	2.5388E-03	9.1144E-04	7.1660E-03	1.7235E-02
3.4	6.1294E-06	3.2212E-03	6.0734E-04	6.4835E-03	1.7917E-02
3.6	5.8825E-06	3.7266E-03	3.1746E-04	5.9780E-03	1.8422E-02
3.8	5.3923E-06	4.1011E-03	7.3334E-05	5.6036E-03	1.8797E-02
4	4.7150E-06	4.3787E-03	1.2245E-04	5.3260E-03	1.9074E-02
4.2	3.9048E-06	4.5846E-03	2.7587E-04	5.1202E-03	1.9280E-02
4.4	3.0112E-06	4.7373E-03	3.9450E-04	4.9675E-03	1.9433E-02
4.6	2.0767E-06	4.8505E-03	4.8537E-04	4.8544E-03	1.9546E-02
4.8	1.1363E-06	4.9346E-03	5.5436E-04	4.7704E-03	1.9630E-02
5	2.1715E-07	4.9969E-03	6.0618E-04	4.7082E-03	1.9692E-02
5.2	6.6068E-07	5.0432E-03	6.4444E-04	4.6621E-03	1.9739E-02
5.4	1.4834E-06	5.0775E-03	6.7177E-04	4.6279E-03	1.9773E-02
5.6	2.2426E-06	5.1030E-03	6.8989E-04	4.6027E-03	1.9798E-02
5.8	2.9339E-06	5.1219E-03	6.9966E-04	4.5840E-03	1.9817E-02
6	3.5563E-06	5.1359E-03	7.0096E-04	4.5703E-03	1.9831E-02

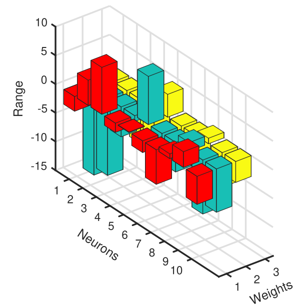

(a) Weights obtained by ANN-BHCS algorithm.

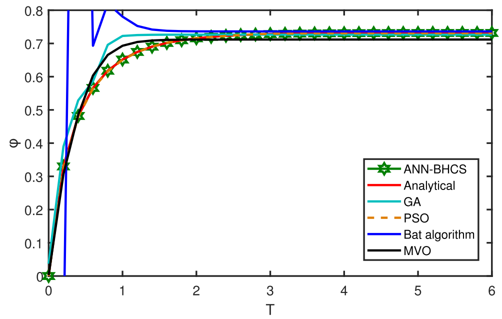

(b) Solution obtained by ANN-BHCS algorithm.

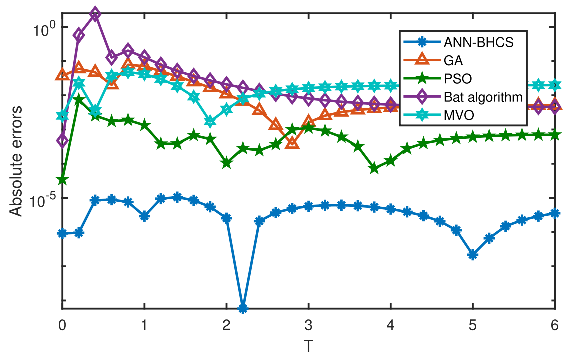

(c) Absolute errors obtained by ANN-BHCS algorithm and other algorithms.

FIGURE 8. **Results obtained by ANN-BHCS algorithm for case 2.**

TABLE 9. **Analysis of the values of performance metrics obtained by ANN-BHCS algorithm for case 2.**

Metrics	Best	Mean	Worst
Fitness	4.2369E-10	1.3492E-04	8.5574E-03
MAD	4.2633E-06	1.1355E-03	3.2206E-02
TIC	1.1689E-06	2.9174E-04	7.7798E-03
ENSE	2.8264E-10	2.2596E-04	1.6129E-02

TABLE 10. **Convergence analysis of performance metrics for case 2.**

Metrics	≤E-03	≤E-04	≤E-05	≤E-06
Fitness	100	98	86	79
MAD	99	80	62	8
TIC	100	91	76	41
ENSE	99	97	88	79

Similarly, a histogram of the ENSE values shows that more than 95% of the values are less than or equal to $E-03$ and

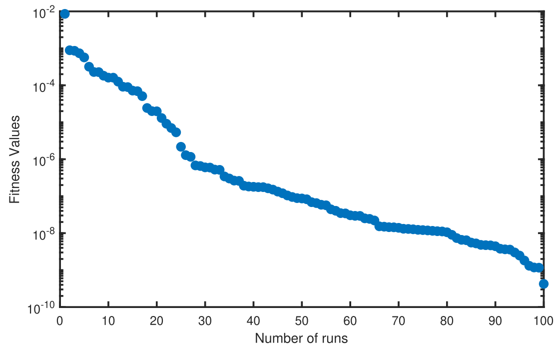

(a) Convergence of the fitness values.

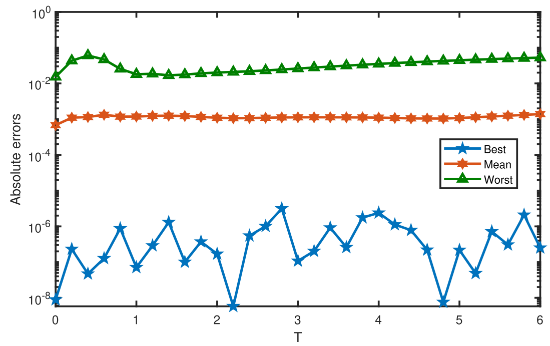

(b) Values of the errors in terms of best, mean and worst .

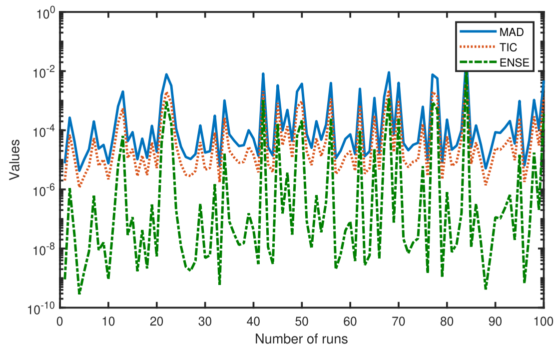

(c) Values of performance metrics.

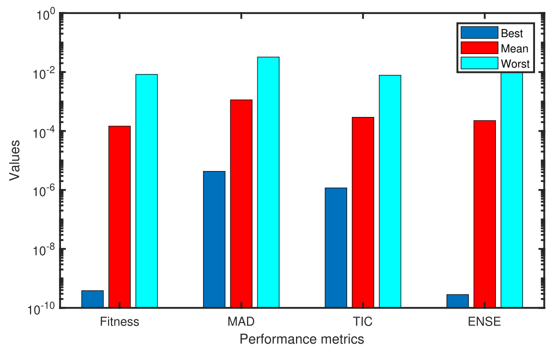

(d) Minimum, mean and maximum values of performance metrics.

FIGURE 9. **Performance analysis of ANN-BHCS algorithm for case 2.**

box plot shows that more than 75% of the values are between $E-06$ to $E-10$. The above results show that ANN-BHCS algorithm can efficiently solve the ODE of case 2.

TABLE 11. Statistical analysis of absolute errors obtained for case 2 by ANN-BHCS algorithm.

T	Min	Mean	SD
0	8.8964E-09	6.8129E-04	2.4459E-03
0.2	2.3107E-07	1.0993E-03	4.5666E-03
0.4	4.7022E-08	1.1478E-03	6.1784E-03
0.6	1.2707E-07	1.3256E-03	5.1287E-03
0.8	8.7080E-07	1.1754E-03	3.6814E-03
1	7.1049E-08	1.1828E-03	3.2130E-03
1.2	2.8884E-07	1.2357E-03	3.3095E-03
1.4	1.3053E-06	1.2489E-03	3.1486E-03
1.6	1.0013E-07	1.2213E-03	3.0607E-03
1.8	3.7131E-07	1.1577E-03	3.0198E-03
2	1.6942E-07	1.0944E-03	3.0231E-03
2.2	5.7879E-09	1.0624E-03	3.0572E-03
2.4	5.4635E-07	1.0691E-03	3.1079E-03
2.6	1.0086E-06	1.0947E-03	3.1709E-03
2.8	3.1475E-06	1.1166E-03	3.2475E-03
3	1.0778E-07	1.1260E-03	3.3373E-03
3.2	2.0243E-07	1.1299E-03	3.4366E-03
3.4	9.1776E-07	1.1281E-03	3.5451E-03
3.6	2.5900E-07	1.1239E-03	3.6620E-03
3.8	1.7517E-06	1.1164E-03	3.7878E-03
4	2.3870E-06	1.1016E-03	3.9237E-03
4.2	1.1210E-06	1.0796E-03	4.0694E-03
4.4	7.7953E-07	1.0507E-03	4.2242E-03
4.6	2.1933E-07	1.0431E-03	4.3805E-03
4.8	7.5727E-09	1.0412E-03	4.5420E-03
5	2.1715E-07	1.0764E-03	4.7012E-03
5.2	4.8397E-08	1.1293E-03	4.8627E-03
5.4	7.1671E-07	1.1876E-03	5.0308E-03
5.6	3.0594E-07	1.2504E-03	5.2101E-03
5.8	2.0905E-06	1.3130E-03	5.4115E-03
6	2.5084E-07	1.3909E-03	5.6538E-03

3) CASE 3

In this case, the values of $\mu_r = 0.2$ and $\beta = 1$. Using these values in Eq.(16) we obtain:

$$\frac{d\varphi}{dT} = (1-\varphi)^2 - 0.2, \tag{43}$$

using Eq.(43), the minimization fitness function for this case is given by:

$$E = \frac{1}{31}\sum_{m=0}^{N}\left(\frac{d\hat{\varphi}}{dT} - \left(1-\hat{\varphi}\right)^2 + 0.2\right)^2 + (\varphi(0)-0)^2. \tag{44}$$

There are 10 neurons in the proposed ANN model. The solution obtained using the ANN-BHCS algorithm contains 10 terms corresponding to the number of neurons. The fitness value obtained for this case is $2.9009E-11$.

The convergence of the fitness values for 100 simulations is plotted in Figure(12a). Weights obtained by the ANN-BHCS algorithm to minimized the fitness function are plotted in Figure(11a). Using these weights, the series solution for Case 3 is given as follows:

$$\begin{aligned}\hat{\varphi}(T) = {} & \frac{-1.38540181566634}{1+e^{-(-0.950574525970029*T-1.18368808365982)}} \\ & + \frac{-8.40788875027298}{1+e^{-(-4.45029347249248*T-5.61345807716124)}} \\ & + \frac{4.53230278396465}{1+e^{-(-0.273007217458138*T-8.06111656372051)}} \\ & + \frac{-1.58437751855973}{1+e^{-(-1.67445265900953*T-2.26618388671243)}} \\ & + \frac{-1.82470604410146}{1+e^{-(-0.764233455895824*T-3.61558826473259)}} \\ & + \frac{-3.90997077413824}{1+e^{-(-17.7806558872269*T-10.9148389014574)}} \\ & + \frac{-29.9988882773316}{1+e^{-(-2.12763433103979*T-5.52774689427097)}} \\ & + \frac{0.552520369343823}{1+e^{-(2.71085606768690*T+3.31637914466232)}} \\ & + \frac{2.41319288267510}{1+e^{-(-1.06174791140192*T-2.81649815996199)}} \\ & + \frac{0.589652764447264}{1+e^{-(0.785176099344001*T-13.8466831300805)}}.\end{aligned} \tag{45}$$

Numerical solutions obtained by the ANN-BHCS algorithm and other algorithms for case 3 are given in Table (12). The solutions are also plotted in Figure (11b).

Absolute errors of the ANN-BHCS algorithm and other algorithms are compared in Table (13) and Figure (11c). From Table (13) and Figure (11c), we can see that ANN-BHCS algorithm gives a solution with minimum absolute errors.

Statistical analysis of the absolute errors is given in Table (16) and minimum, mean and maximum values of absolute errors are also plotted in Figure (12b). The minimum values of absolute errors are in range $E-07$ to $E-09$, mean values are in range $E-03$ to $E-04$, and standard deviation range from $E-03$ to $E-04$. The statistical analysis of absolute errors shows the accuracy in the solutions obtained by the ANN-BHCS algorithm. The values of performance metrics for 100 runs are plotted in Figure (12c).

The values of performance metrics and fitness function in terms of best, mean and worst are presented in Table (14) and are also shown in Figure (12d). Convergence analysis of fitness values and performance metrics are given in Table (15).

Histograms and box plots of fitness values and performance metrics are presented in Figure (13). Histogram of the fitness values shows that 100% of the values are less than or equal to $E-03$ and the box plot of the fitness values shows that more than 75% of the values are in the range $E-07$ to $E-11$. Histogram of the MAD values shows that more than 95% of the values are less than or equal to $E-03$ and the box plot shows that more than 75% of the values are in the range $E-04$ to $E-06$. Histogram of TIC values shows that 95% of the values are less than or equal to $E-03$ and the box plot shows that more than 75% of the values are between $E-05$ and $E-07$. Histogram of the ENSE values shows that more than 95% of the values are less than or equal to $E-03$ and the box plot shows that more than 75% of the values are in

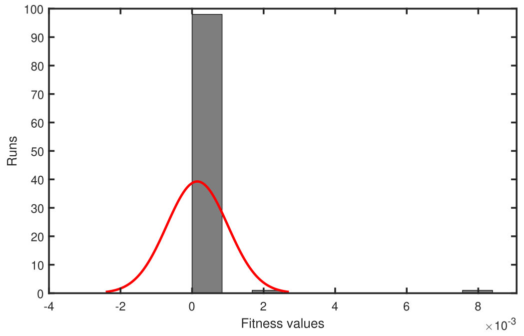

(a) Histogram for fitness values.

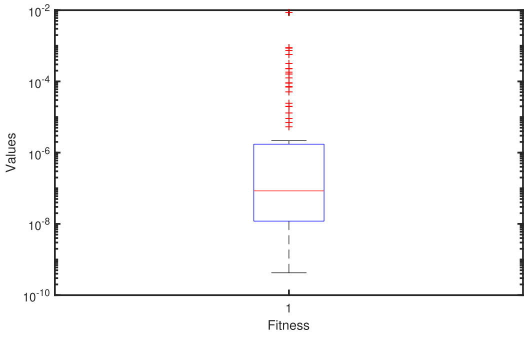

(b) Box plot for fitness values.

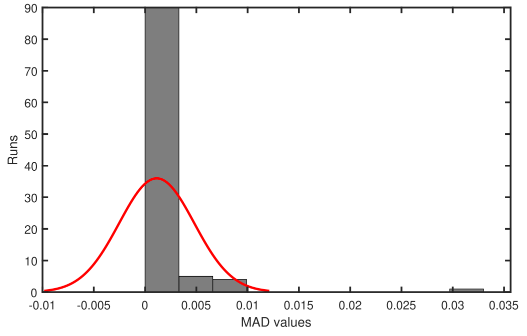

(c) Histogram for MAD values.

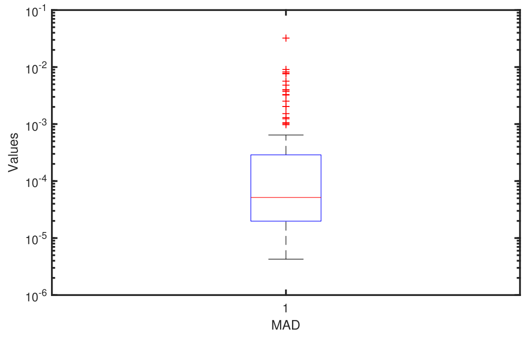

(d) Box plot for MAD values.

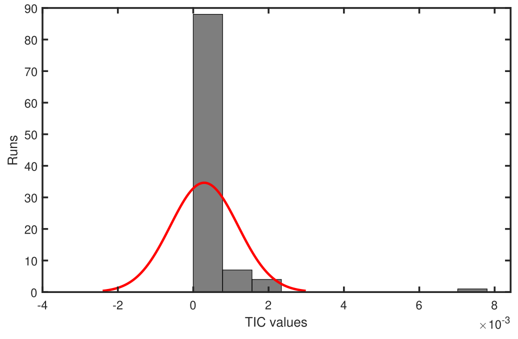

(e) Histogram for TIC values.

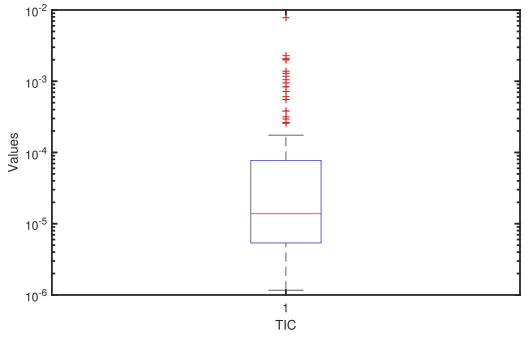

(f) Box plot for TIC values.

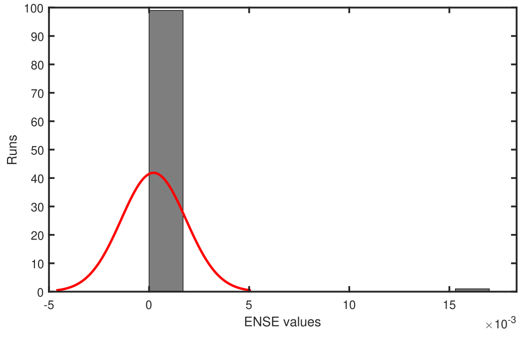

(g) Histogram for ENSE values.

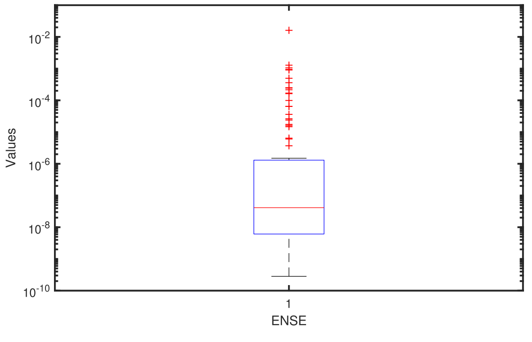

(h) Box plot for ENSE values.

FIGURE 10. Histograms and box plots of values of performance metrics for case 2.

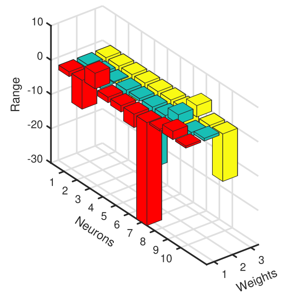

(a) Weights obtained by ANN-BHCS algorithm.

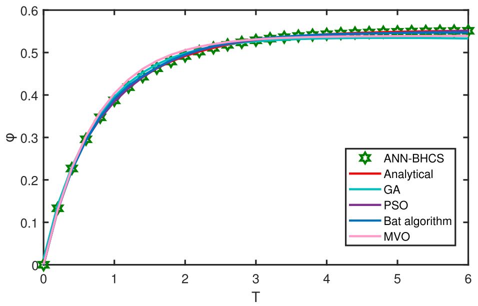

(b) Solution obtained by ANN-BHCS algorithm.

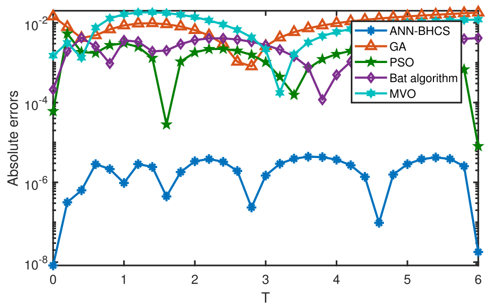

(c) Absolute errors obtained by ANN-BHCS algorithm and other algorithms.

FIGURE 11. Results obtained by ANN-BHCS algorithm for case 3.

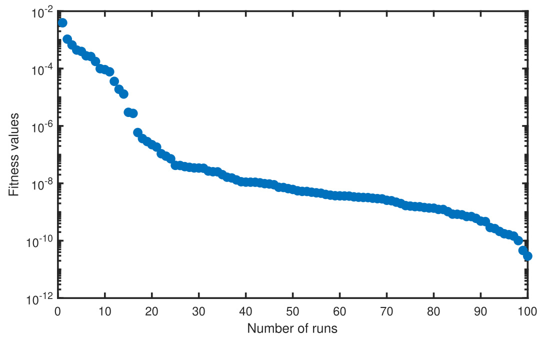

(a) Convergence of the fitness values.

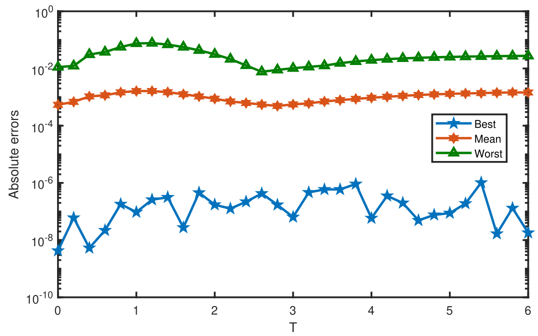

(b) Best, mean and worst values of errors.

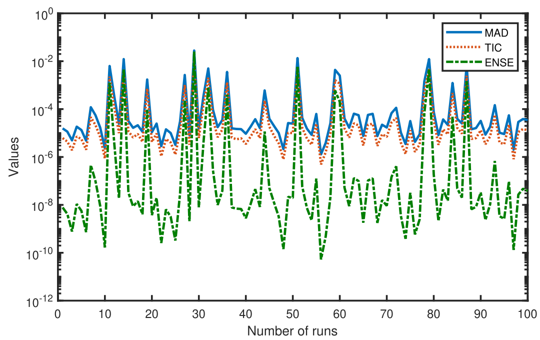

(c) Values of performance metrics.

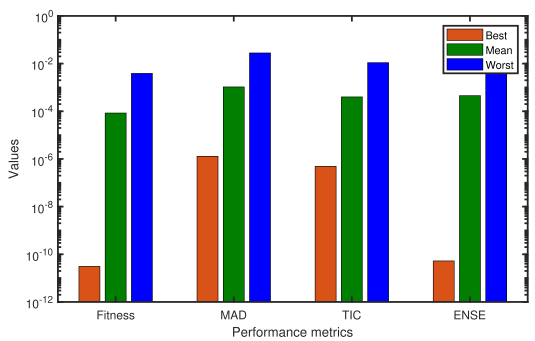

(d) Minimum, mean and maximum values of performance metrics.

FIGURE 12. Performance analysis of ANN-BHCS algorithm for case 3.

the range $E-07$ to $E-11$. The results of case 3 show the accuracy and efficiency of the ANN-BHCS algorithm.

4) CASE 4

In this case, the values of $\mu_r = 0.6$ and $\beta = 0.2$. Using these values, Eq.(16) becomes

$$\frac{d\varphi}{dT} = \left(\frac{1-\varphi}{0.2}\right)^2 - 0.6, \tag{46}$$

using Eq.(46), the minimization fitness function for this case is written as:

$$E = \frac{1}{31}\sum_{m=0}^{N}\left(\frac{d\hat{\varphi}}{dT} - \left(\frac{1-\hat{\varphi}}{0.2}\right)^2 + 0.6\right)^2 + (\varphi(0)-0)^2. \tag{47}$$

The fitness value obtained for this case is $5.2611E-08$. Convergence of the fitness values for 100 runs is given in Figure(15a). Weights obtained to minimize the fitness function are given in Figure(14a). Using these weights, the series solution for this case is given as:

$$\hat{\varphi}(T) = \frac{20.7552214809028}{1+e^{-(-29.9987356047387*T-1.46100865967742)}}$$

TABLE 12. Solutions obtained for case 3.

T	Analytical [24]	ANN-BHCS	GA	PSO	Bat algorithm	MVO
0	0.0000000	0.0000000	0.0143796	0.0000607	0.0002112	0.0014994
0.2	0.1330379	0.1330375	0.1408305	0.1276853	0.1310819	0.1299099
0.4	0.2268467	0.2268474	0.2309834	0.2250038	0.2226388	0.2281745
0.6	0.2955873	0.2955845	0.3004389	0.2938335	0.2930317	0.3031513
0.8	0.3473905	0.3473884	0.3542178	0.3446439	0.3483446	0.3602322
1	0.3872602	0.3872612	0.3958372	0.3841886	0.3908768	0.4036152
1.2	0.4184454	0.4184483	0.4280212	0.4159681	0.4218088	0.4365449
1.4	0.4431476	0.4431500	0.4528910	0.4418347	0.4450653	0.4615156
1.6	0.4629108	0.4629113	0.4720966	0.4628827	0.4649273	0.4804371
1.8	0.4788492	0.4788474	0.4869185	0.4799131	0.4817747	0.4947666
2	0.4917860	0.4917826	0.4983497	0.4935984	0.4954771	0.5056140
2.2	0.5023413	0.5023374	0.5071591	0.5045271	0.5064068	0.5138227
2.4	0.5109902	0.5109869	0.5139413	0.5132122	0.5150656	0.5200332
2.6	0.5181018	0.5180999	0.5191561	0.5200924	0.5219088	0.5247309
2.8	0.5239662	0.5239659	0.5231583	0.5255357	0.5273122	0.5282839
3	0.5288134	0.5288149	0.5262219	0.5298455	0.5315767	0.5309709
3.2	0.5328278	0.5328307	0.5285580	0.5332683	0.5349415	0.5330027
3.4	0.5361577	0.5361617	0.5303293	0.5360023	0.5375960	0.5345390
3.6	0.5389237	0.5389281	0.5316610	0.5382059	0.5396899	0.5357005
3.8	0.5412237	0.5412280	0.5326489	0.5400047	0.5413413	0.5365788
4	0.5431381	0.5431418	0.5333668	0.5414984	0.5426437	0.5372428
4.2	0.5447327	0.5447354	0.5338707	0.5427656	0.5436708	0.5377448
4.4	0.5460618	0.5460632	0.5342032	0.5438689	0.5444807	0.5381243
4.6	0.5471702	0.5471701	0.5343964	0.5448580	0.5451194	0.5384112
4.8	0.5480950	0.5480934	0.5344741	0.5457730	0.5456230	0.5386281
5	0.5488668	0.5488639	0.5344537	0.5466462	0.5460201	0.5387921
5.2	0.5495112	0.5495073	0.5343474	0.5475044	0.5463331	0.5389161
5.4	0.5500493	0.5500451	0.5341633	0.5483701	0.5465800	0.5390098
5.6	0.5504988	0.5504949	0.5339064	0.5492627	0.5467746	0.5390806
5.8	0.5508743	0.5508717	0.5335787	0.5501995	0.5469281	0.5391342
6	0.5511880	0.5511881	0.5331799	0.5511961	0.5470491	0.5391747

TABLE 13. Comparison of absolute errors of ANN-BHCS algorithm and other algorithms for case 3.

T	ANN-BHCS	GA	PSO	Bat algorithm	MVO
0	8.2638E-09	1.4380E-02	6.0705E-05	2.1124E-04	1.4994E-03
0.2	3.1557E-07	7.7926E-03	5.3526E-03	1.9559E-03	3.1279E-03
0.4	6.3168E-07	4.1367E-03	1.8430E-03	4.2079E-03	1.3277E-03
0.6	2.8589E-06	4.8516E-03	1.7539E-03	2.5557E-03	7.5640E-03
0.8	2.1525E-06	6.8272E-03	2.7466E-03	9.5406E-04	1.2842E-02
1	9.6490E-07	8.5770E-03	3.0716E-03	3.6166E-03	1.6355E-02
1.2	2.8702E-06	9.5757E-03	2.4773E-03	3.3634E-03	1.8099E-02
1.4	2.4330E-06	9.7434E-03	1.3129E-03	1.9177E-03	1.8368E-02
1.6	4.4347E-07	9.1857E-03	2.8140E-05	2.0165E-03	1.7526E-02
1.8	1.8105E-06	8.0693E-03	1.0639E-03	2.9255E-03	1.5917E-02
2	3.3750E-06	6.5638E-03	1.8124E-03	3.6911E-03	1.3828E-02
2.2	3.8465E-06	4.8178E-03	2.1858E-03	4.0656E-03	1.1481E-02
2.4	3.2682E-06	2.9511E-03	2.2220E-03	4.0754E-03	9.0430E-03
2.6	1.9367E-06	1.0542E-03	1.9905E-03	3.8070E-03	6.6291E-03
2.8	2.3441E-07	8.0787E-04	1.5696E-03	3.3460E-03	4.3178E-03
3	1.4806E-06	2.5915E-03	1.0321E-03	2.7633E-03	2.1575E-03
3.2	2.9295E-06	4.2697E-03	4.4049E-04	2.1137E-03	1.7488E-04
3.4	3.9302E-06	5.8284E-03	1.5546E-04	1.4383E-03	1.6188E-03
3.6	4.3919E-06	7.2627E-03	7.1784E-04	7.6616E-04	3.2232E-03
3.8	4.3010E-06	8.5748E-03	1.2190E-03	1.1756E-04	4.6450E-03
4	3.7031E-06	9.7713E-03	1.6398E-03	4.9440E-04	5.8953E-03
4.2	2.6874E-06	1.0862E-02	1.9671E-03	1.0619E-03	6.9879E-03
4.4	1.3736E-06	1.1859E-02	2.1929E-03	1.5811E-03	7.9375E-03
4.6	9.6615E-08	1.2774E-02	2.3122E-03	2.0508E-03	8.7590E-03
4.8	1.5663E-06	1.3621E-02	2.3220E-03	2.4720E-03	9.4668E-03
5	2.8656E-06	1.4413E-02	2.2206E-03	2.8467E-03	1.0075E-02
5.2	3.8136E-06	1.5164E-02	2.0068E-03	3.1780E-03	1.0595E-02
5.4	4.2164E-06	1.5886E-02	1.6792E-03	3.4693E-03	1.1039E-02
5.6	3.8663E-06	1.6592E-02	1.2361E-03	3.7241E-03	1.1418E-02
5.8	2.5374E-06	1.7296E-02	6.7482E-04	3.9462E-03	1.1740E-02
6	1.7988E-08	1.8008E-02	8.0470E-06	4.1389E-03	1.2013E-02

$$+\frac{10.7556967111483}{1+e^{-(-29.9794310928430*T-16.8737833756299)}}$$
$$+\frac{-29.5031465383362}{1+e^{-(-1.74013235006156*T-18.2955983404539)}}$$

TABLE 14. Analysis of the performance metrics obtained by ANN-BHCS algorithm for case 3.

Metrics	Best	Mean	Worst
Fitness	2.9009E-11	7.5647E-05	3.9405E-03
MAD	1.2864E-06	1.0494E-03	2.7953E-02
TIC	4.8866E-07	3.9976E-04	1.0968E-02
ENSE	5.2577E-11	4.5241E-04	2.4827E-02

TABLE 15. Convergence analysis of performance metrics for case 3.

Metrics	≤E-03	≤E-04	≤E-05	≤E-06
Fitness	100	98	91	86
MAD	96	86	80	20
TIC	99	89	83	55
ENSE	99	94	89	85

$$+\frac{-29.9911571516672}{1+e^{-(-29.9997568021939*T-3.86417253453530)}}$$
$$+\frac{-0.193227460333962}{1+e^{-(29.6079673117902*T+6.00997081549918)}}$$
$$+\frac{-2.47238436924293}{1+e^{-(-28.2021836982231*T-2.98565931953008)}}$$
$$+\frac{-29.9834111563651}{1+e^{-(-28.0770690781443*T-4.55393749085514)}}$$
$$+\frac{-29.5565828111271}{1+e^{-(-28.6716114631666*T-2.00818674949371)}}$$

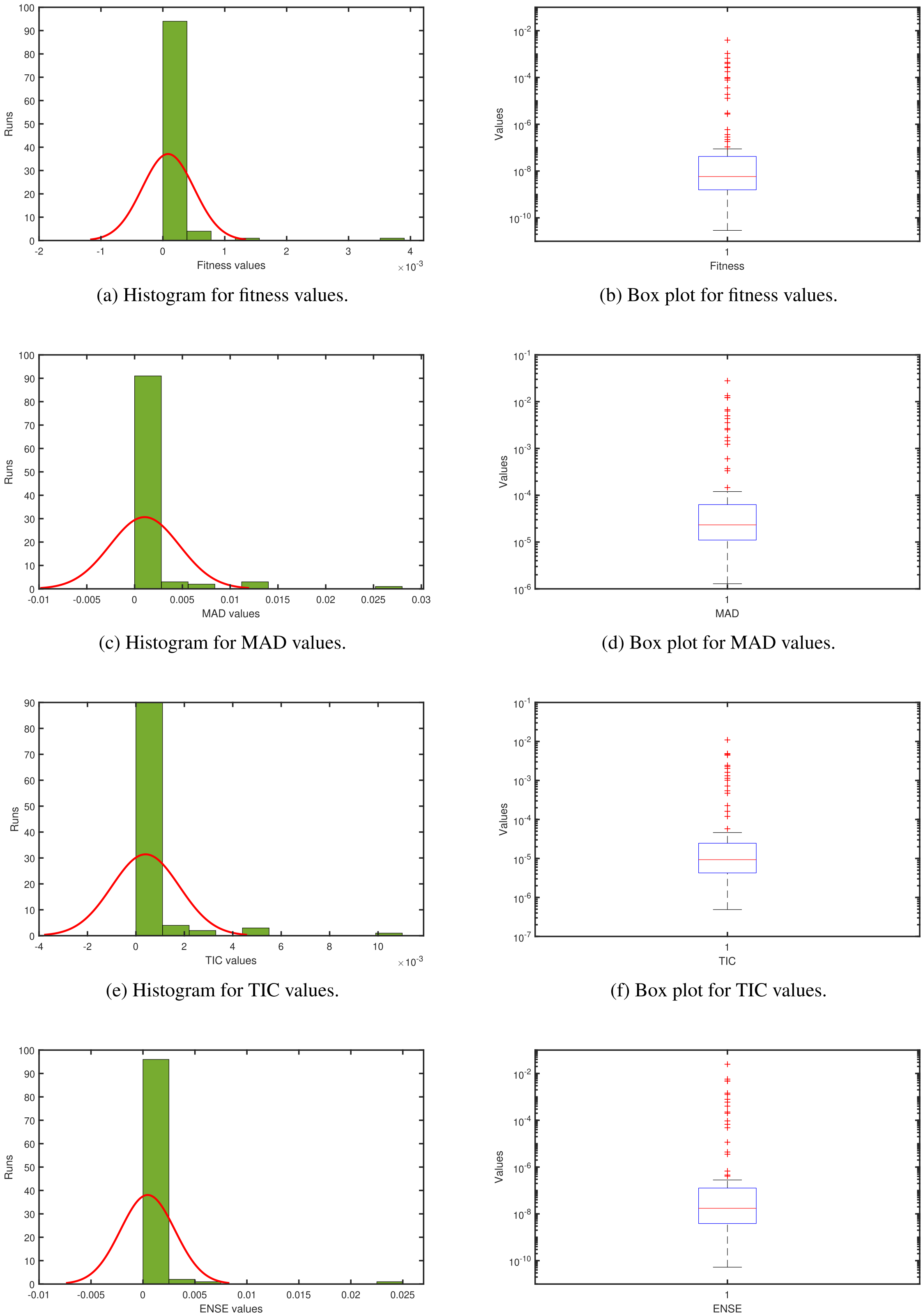

(a) Histogram for fitness values.
(b) Box plot for fitness values.
(c) Histogram for MAD values.
(d) Box plot for MAD values.
(e) Histogram for TIC values.
(f) Box plot for TIC values.
(g) Histogram for ENSE values.
(h) Box plot for ENSE values.

FIGURE 13. **Histograms and box plots of values of performance metrics for case 3.**

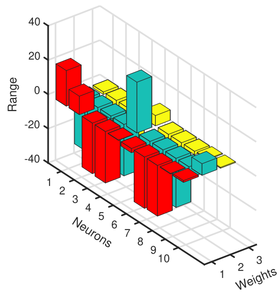

(a) Weights obtained by ANN-BHCS algorithm.

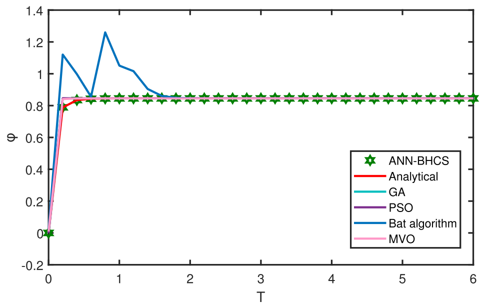

(b) Solution obtained by ANN-BHCS algorithm.

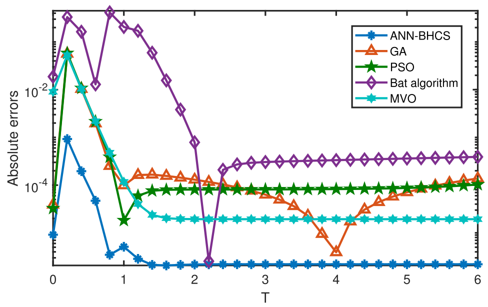

(c) Absolute errors obtained by ANN-BHCS algorithm and other algorithms.

FIGURE 14. Results obtained by ANN-BHCS algorithm for case 4.

$$+\frac{0.289552983688114}{1+e^{-(-6.61346781045494*T+0.463606898473104)}}$$
$$+\frac{1.03830592809746}{1+e^{-(6.75364590521670*T+0.523037857571163)}}. \quad (48)$$

Numerical solutions obtained by ANN-BHCS algorithm and other algorithms for case 4 are presented in Table(17). The solutions are also plotted in Figure(14b). Absolute errors of the ANN-BHCS algorithm and other algorithms are compared in Table (18) and Figure (14c) which shows that the ANN-BHCS algorithm can obtain a solution with less absolute errors than other algorithms.

Statistical analysis of absolute errors of the ANN-BHCS algorithm is given in Table(21) and minimum, mean and maximum values of absolute errors are also plotted in Figure(15b). The minimum values of absolute errors are in the range $E-04$ to $E-08$, mean values are in the range $E-02$ to $E-04$ and standard deviation (SD) is in the range $E-02$ to $E-03$ which shows the accuracy in the solutions obtained by the ANN-BHCS algorithm.

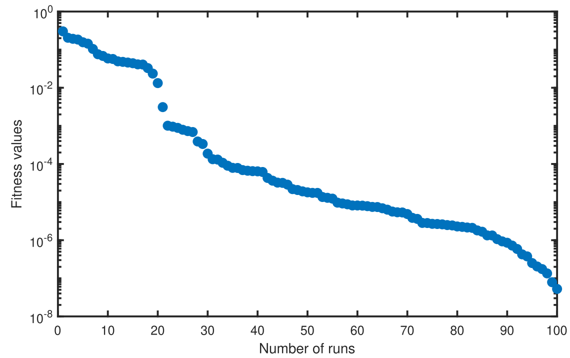

(a) Convergence of the fitness values.

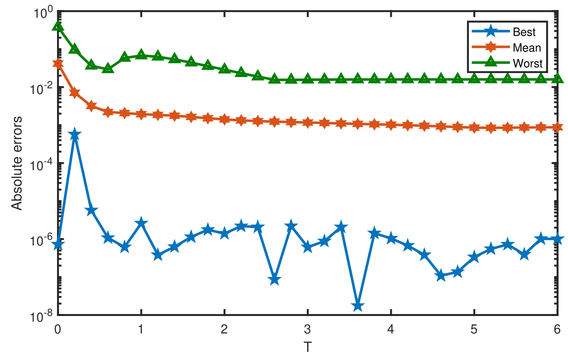

(b) Best, mean and worst values of errors.

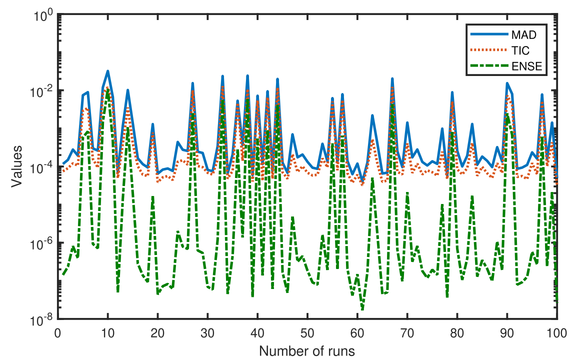

(c) Values of performance metrics.

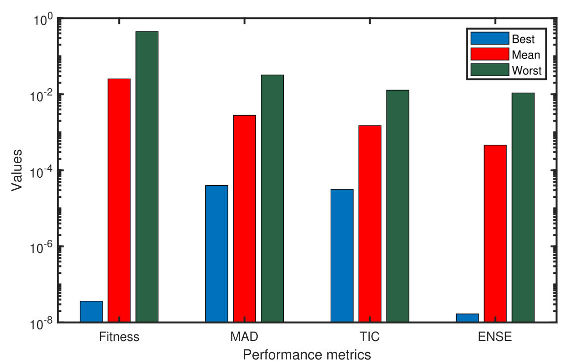

(d) Minimum, mean and maximum values of performance metrics.

FIGURE 15. Performance analysis of ANN-BHCS algorithm for case 4.

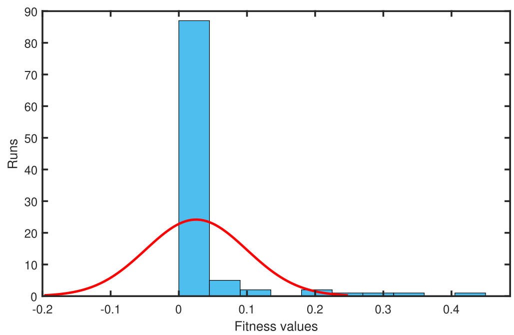

(a) Histogram for fitness values.

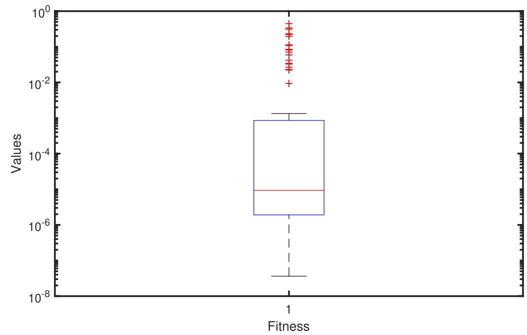

(b) Box plot for fitness values.

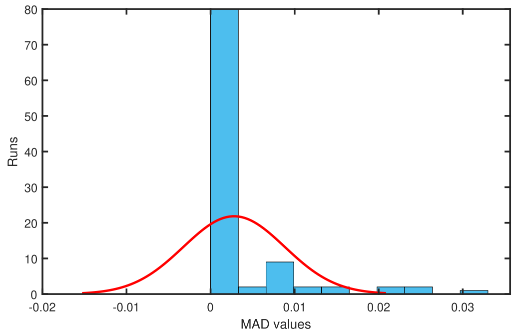

(c) Histogram for MAD values.

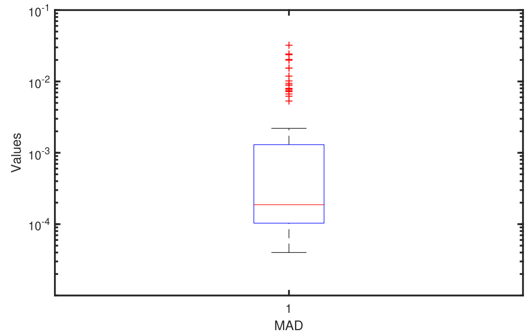

(d) Box plot for MAD values.

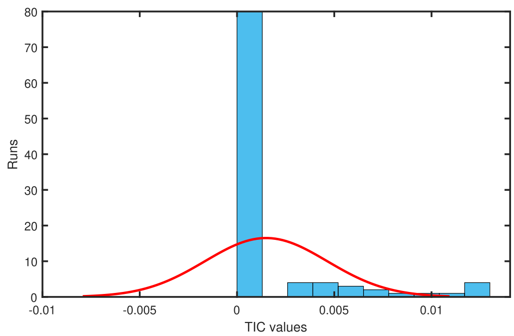

(e) Histogram for TIC values.

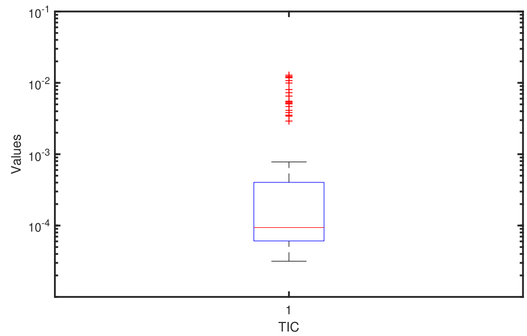

(f) Box plot for TIC values.

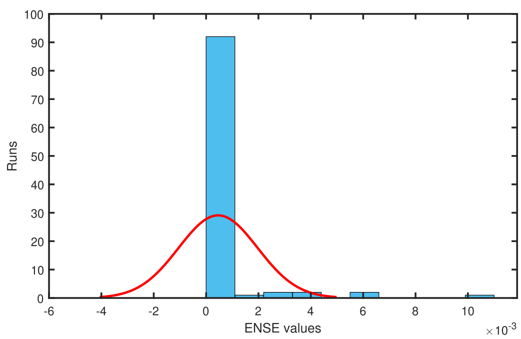

(g) Histogram for ENSE values.

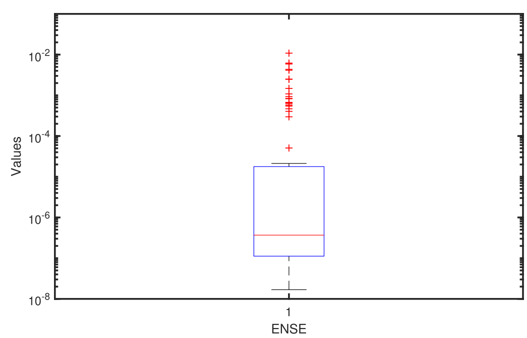

(h) Box plot for ENSE values.

FIGURE 16. Histograms and box plots of values of performance metrics for case 4.

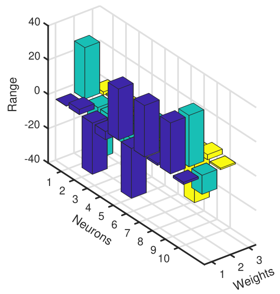

(a) Weights obtained by ANN-BHCS algorithm.

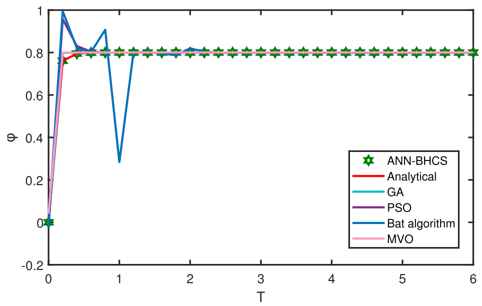

(b) Solution obtained by ANN-BHCS algorithm.

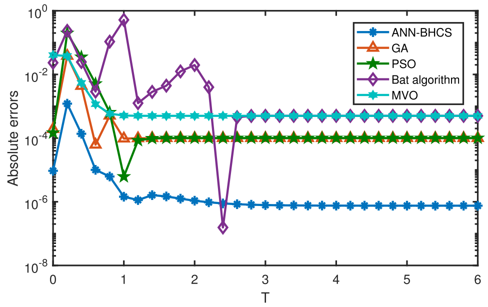

(c) Absolute errors obtained by ANN-BHCS algorithm and other algorithms.

FIGURE 17. Results obtained by ANN-BHCS algorithm for case 5.

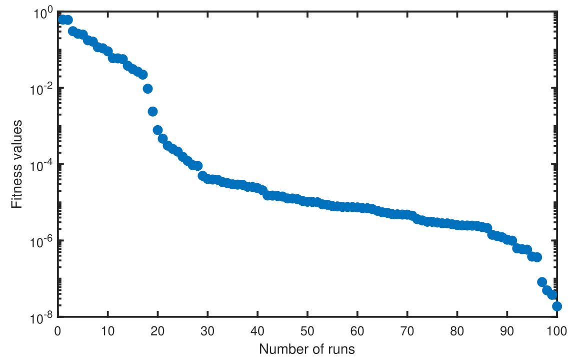

(a) Convergence of the fitness values.

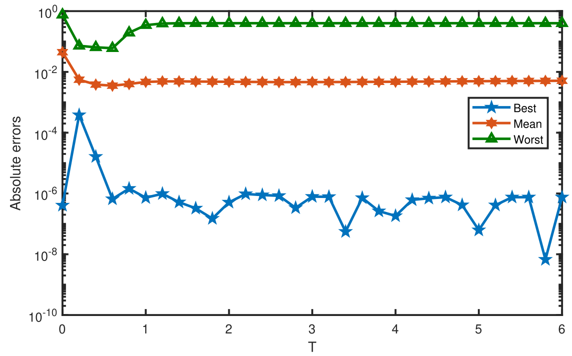

(b) Best, mean and worst values of errors.

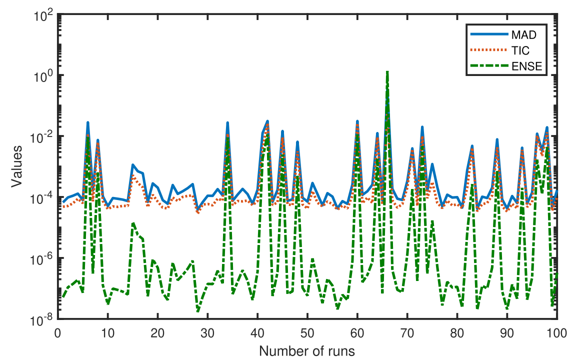

(c) Values of performance metrics.

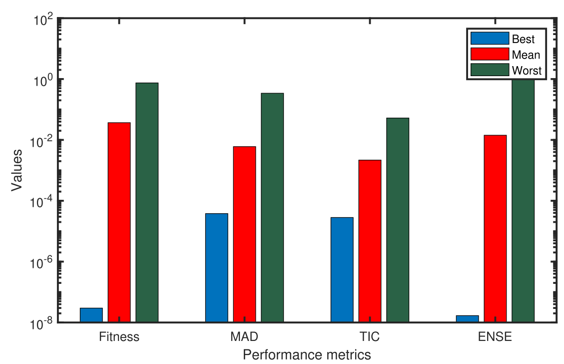

(d) Minimum, mean and maximum values of performance metrics.

FIGURE 18. Performance analysis of ANN-BHCS algorithm for case 5.

The values of performance metrics for 100 runs are plotted in Figure(15c). The minimum, mean and maximum values of the performance metrics and fitness function are given in Table(19) and are also plotted in Figure(15d). Convergence analysis of the fitness values and performance metrics is presented in Table (20).

Histograms and box plots of the values of the fitness function and performance metrics are given in Figure(16). Histogram of the fitness values shows that more than 80% of the values are less than or equal to $E-03$ and the box plot shows that more than 75% of the values are in the range $E-03$ to $E-08$. Histogram of the MAD values shows that over 90% of the values are less than or equal to $E-03$ and the box plot shows that more than 75% of the values are in the $E-03$ to $E-05$. Histogram of TIC values shows that more than 90% of the values are less than or equal to $E-03$ and the box plot shows that more than 75% of the values are in the range $E-04$ to $E-05$. Histogram for ENSE values shows that more than 95% of the values are less than or equal to $E-03$ and the box plot shows that more than 75% of the

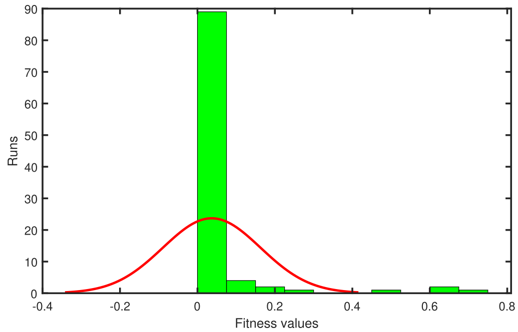

(a) Histogram for fitness values.

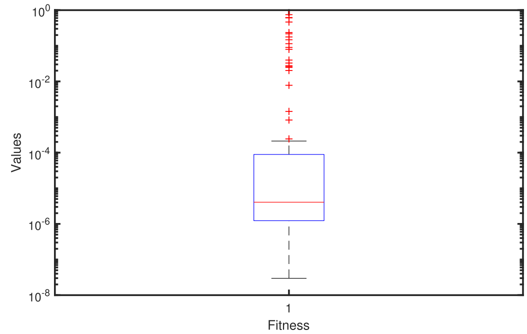

(b) Box plot for fitness values.

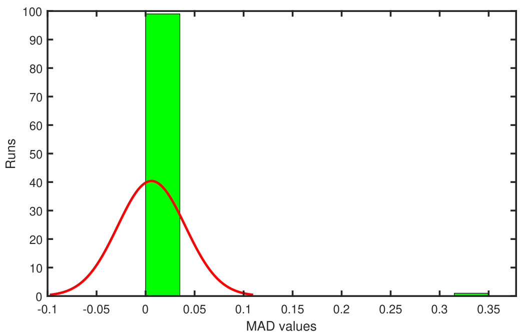

(c) Histogram for MAD values.

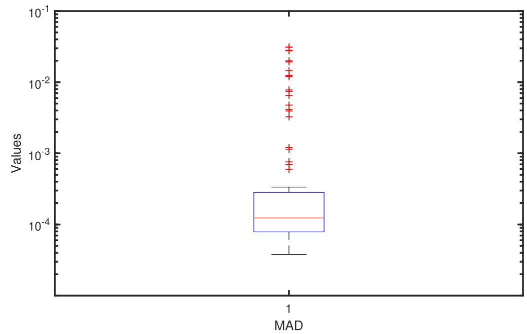

(d) Box plot for MAD values.

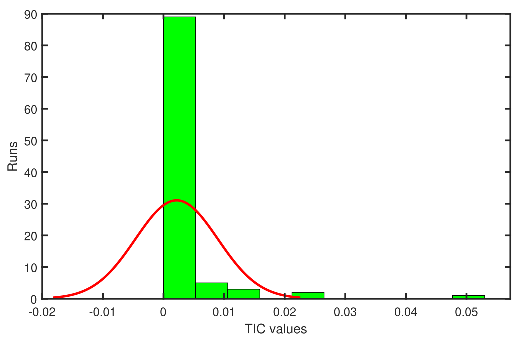

(e) Histogram for TIC values.

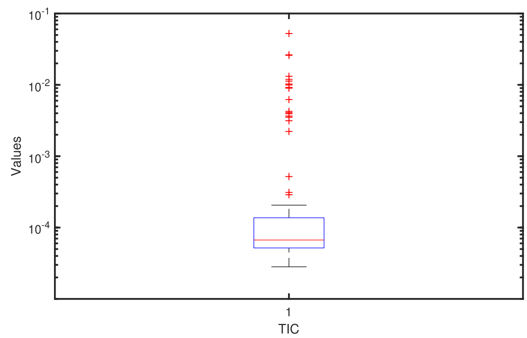

(f) Box plot for TIC values.

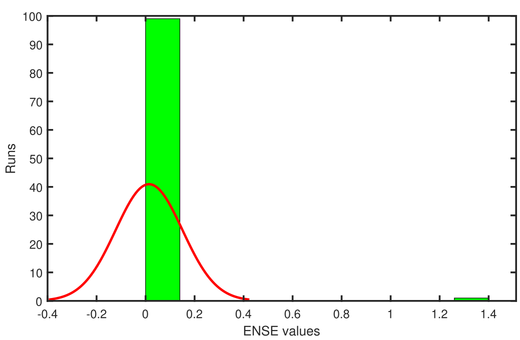

(g) Histogram for ENSE values.

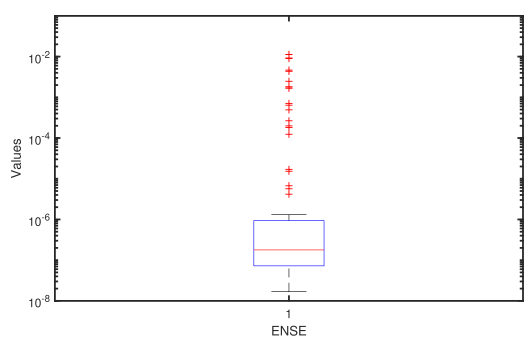

(h) Box plot for ENSE values.

FIGURE 19. Histograms and box plots of values of performance metrics for case 5.

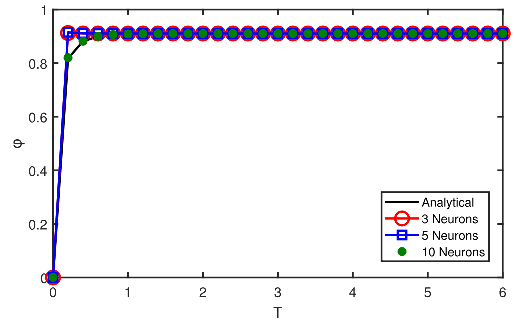

(a) Solutions obtained by ANN-BHCS algorithm.

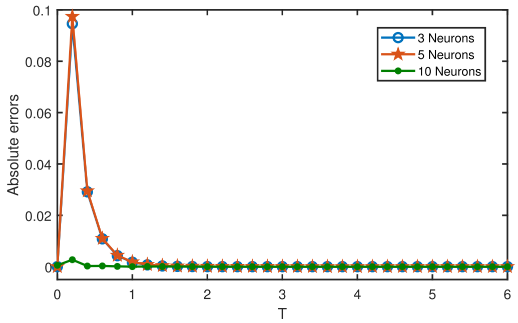

(b) Absolute errors in solutions.

FIGURE 20. Results obtained for different number of neurons.

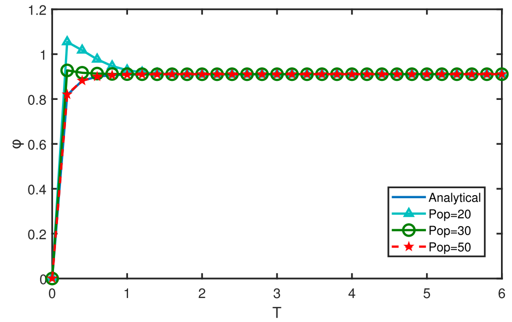

(a) Solutions obtained by ANN-BHCS algorithm.

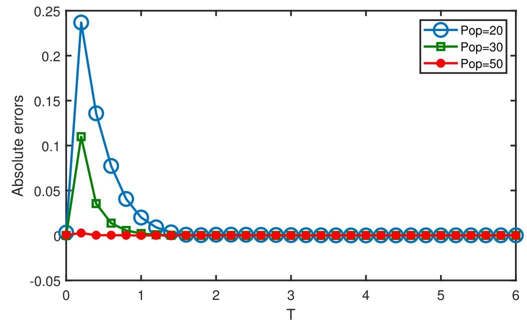

(b) Absolute errors in solutions.

FIGURE 21. Results obtained for different population sizes.

values are between $E-05$ and $E-08$. These results for case 4 show the efficiency of the ANN-BHCS algorithm.

5) CASE 5

In this case, the values of $\mu_r = 1$ and $\beta = 0.2$. Using these values, Eq.(16) becomes

$$\frac{d\varphi}{dT} = \left(\frac{1-\varphi}{0.2}\right)^2 - 1, \tag{49}$$

using Eq.(49), the minimization objective function for this case can be written as:

$$E = \frac{1}{31}\sum_{m=0}^{N}\left(\frac{d\hat{\varphi}}{dT} - \left(\frac{1-\hat{\varphi}}{0.2}\right)^2 + 1\right)^2 + (\varphi(0)-0)^2. \tag{50}$$

Numerical solutions obtained by the ANN-BHCS algorithm and other algorithms for case 5 are presented in Table(22) and solutions are also plotted in Figure(17b).

The absolute errors of the ANN-BHCS algorithm are compared with other algorithms in Table (23) and Figure (17c). The absolute errors of the ANN-BHCS algorithm are less than that of other algorithms which shows that solution obtained by the ANN-BHCS algorithm is better than other algorithms. Statistical analysis of absolute errors of the ANN-BHCS algorithm is given in Table(26) and minimum, mean, and maximum values of absolute errors are also plotted in Figure(18b). The minimum values of absolute errors are in the range $E-04$ to $E-09$, mean values are in the range $E-02$ to $E-03$ and standard deviation (SD) is in the range $E-01$ to $E-02$ which shows the accuracy of the ANN-BHCS algorithm solutions.

TABLE 16. Statistical analysis of absolute errors for case 3 obtained by ANN-BHCS algorithm.

T	Min	Mean	SD
0	4.2514E-09	5.3629E-04	5.3629E-04
0.2	6.0303E-08	6.8074E-04	6.8074E-04
0.4	5.2971E-09	1.0531E-03	1.0531E-03
0.6	2.1915E-08	1.1552E-03	1.1552E-03
0.8	1.8042E-07	1.4634E-03	1.4634E-03
1	9.5040E-08	1.6243E-03	1.6243E-03
1.2	2.5782E-07	1.6278E-03	1.6278E-03
1.4	3.1292E-07	1.4827E-03	1.4827E-03
1.6	2.7407E-08	1.2589E-03	1.2589E-03
1.8	4.5467E-07	1.0550E-03	1.0550E-03
2	1.7247E-07	8.7610E-04	8.7610E-04
2.2	1.2551E-07	7.0539E-04	7.0539E-04
2.4	2.1892E-07	6.2030E-04	6.2030E-04
2.6	4.2534E-07	5.4977E-04	5.4977E-04
2.8	1.7064E-07	4.9034E-04	4.9034E-04
3	6.3966E-08	5.5360E-04	5.5360E-04
3.2	4.6403E-07	6.0436E-04	6.0436E-04
3.4	5.9018E-07	7.0320E-04	7.0320E-04
3.6	5.9051E-07	7.8426E-04	7.8426E-04
3.8	9.1353E-07	8.6471E-04	8.6471E-04
4	5.8414E-08	9.4718E-04	9.4718E-04
4.2	3.5246E-07	1.0262E-03	1.0262E-03
4.4	1.9864E-07	1.1084E-03	1.1084E-03
4.6	4.8834E-08	1.1828E-03	1.1828E-03
4.8	7.6000E-08	1.2446E-03	1.2446E-03
5	8.7902E-08	1.2967E-03	1.2967E-03
5.2	1.8924E-07	1.3405E-03	1.3405E-03
5.4	1.0190E-06	1.3769E-03	1.3769E-03
5.6	1.6662E-08	1.4218E-03	1.4218E-03
5.8	1.3109E-07	1.4486E-03	1.4486E-03
6	1.7988E-08	1.4492E-03	1.4492E-03

TABLE 17. Solutions obtained for case 4.

T	Analytical [24]	ANN-BHCS	GA	PSO	Bat algorithm	MVO
0	0.00000000	0.00000915	-0.00003893	-0.00003268	0.01874242	0.00902384
0.2	0.78805881	0.78898340	0.84452667	0.84622680	1.12052602	0.84099467
0.4	0.83450151	0.83469749	0.84484339	0.84526663	0.99784779	0.84488107
0.6	0.84289230	0.84293936	0.84485683	0.84504426	0.85578288	0.84507627
0.8	0.84461839	0.84461491	0.84487022	0.84500646	1.25995686	0.84509735
1	0.84498258	0.84497747	0.84488361	0.84500089	1.05105920	0.84509970
1.2	0.84505984	0.84505698	0.84489701	0.84500007	1.01621334	0.84509997
1.4	0.84507624	0.84507411	0.84491040	0.84499994	0.90441619	0.84510000
1.6	0.84507973	0.84507765	0.84492380	0.84499990	0.86071076	0.84510000
1.8	0.84508047	0.84507833	0.84493720	0.84499987	0.84889834	0.84510000
2	0.84508062	0.84507845	0.84495060	0.84499983	0.84586805	0.84510000
2.2	0.84508066	0.84507846	0.84496399	0.84499978	0.84508320	0.84510000
2.4	0.84508066	0.84507847	0.84497739	0.84499972	0.84487136	0.84510000
2.6	0.84508067	0.84507847	0.84499079	0.84499964	0.84480879	0.84510000
2.8	0.84508067	0.84507847	0.84500419	0.84499955	0.84478663	0.84510000
3	0.84508067	0.84507847	0.84501759	0.84499942	0.84477602	0.84510000
3.2	0.84508067	0.84507847	0.84503099	0.84499926	0.84476897	0.84510000
3.4	0.84508067	0.84507847	0.84504439	0.84499906	0.84476308	0.84510000
3.6	0.84508067	0.84507847	0.84505778	0.84499880	0.84475760	0.84510000
3.8	0.84508067	0.84507847	0.84507118	0.84499847	0.84475222	0.84510000
4	0.84508067	0.84507847	0.84508458	0.84499804	0.84474687	0.84510000
4.2	0.84508067	0.84507847	0.84509798	0.84499750	0.84474148	0.84510000
4.4	0.84508067	0.84507847	0.84511138	0.84499681	0.84473605	0.84510000
4.6	0.84508067	0.84507847	0.84512479	0.84499594	0.84473055	0.84510000
4.8	0.84508067	0.84507847	0.84513819	0.84499481	0.84472500	0.84510000
5	0.84508067	0.84507847	0.84515159	0.84499338	0.84471938	0.84510000
5.2	0.84508067	0.84507847	0.84516499	0.84499156	0.84471369	0.84510000
5.4	0.84508067	0.84507847	0.84517839	0.84498922	0.84470794	0.84510000
5.6	0.84508067	0.84507847	0.84519179	0.84498625	0.84470212	0.84510000
5.8	0.84508067	0.84507847	0.84520519	0.84498246	0.84469623	0.84510000
6	0.84508067	0.84507847	0.84521859	0.84497761	0.84469027	0.84510000

TABLE 18. Comparison of absolute errors of ANN-BHCS algorithm and other algorithms for case 4.

T	ANN-BHCS	GA	PSO	Bat algorithm	MVO
0	9.1529E-06	3.8934E-05	3.2678E-05	1.8742E-02	9.0238E-03
0.2	9.2459E-04	5.6468E-02	5.8168E-02	3.3247E-01	5.2936E-02
0.4	1.9598E-04	1.0342E-02	1.0765E-02	1.6335E-01	1.0380E-02
0.6	4.7059E-05	1.9645E-03	2.1520E-03	1.2891E-02	2.1840E-03
0.8	3.4760E-06	2.5183E-04	3.8808E-04	4.1534E-01	4.7896E-04
1	5.1151E-06	9.8973E-05	1.8303E-05	2.0608E-01	1.1712E-04
1.2	2.8565E-06	1.6283E-04	5.9766E-05	1.7115E-01	4.0130E-05
1.4	2.1354E-06	1.6584E-04	7.6305E-05	5.9340E-02	2.3754E-05
1.6	2.0777E-06	1.5593E-04	7.9828E-05	1.5631E-02	2.0274E-05
1.8	2.1341E-06	1.4327E-04	8.0600E-05	3.8179E-03	1.9533E-05
2	2.1747E-06	1.3003E-04	8.0795E-05	7.8743E-04	1.9376E-05
2.2	2.1928E-06	1.1666E-04	8.0875E-05	2.5480E-06	1.9343E-05
2.4	2.1990E-06	1.0327E-04	8.0942E-05	2.0931E-04	1.9336E-05
2.6	2.2005E-06	8.9876E-05	8.1021E-05	2.7187E-04	1.9334E-05
2.8	2.2005E-06	7.6478E-05	8.1119E-05	2.9404E-04	1.9334E-05
3	2.2001E-06	6.3079E-05	8.1244E-05	3.0465E-04	1.9334E-05
3.2	2.1997E-06	4.9680E-05	8.1404E-05	3.1170E-04	1.9334E-05
3.4	2.1993E-06	3.6281E-05	8.1608E-05	3.1758E-04	1.9334E-05
3.6	2.1991E-06	2.2881E-05	8.1868E-05	3.2307E-04	1.9334E-05
3.8	2.1989E-06	9.4818E-06	8.2199E-05	3.2844E-04	1.9334E-05
4	2.1988E-06	3.9181E-06	8.2622E-05	3.3380E-04	1.9334E-05
4.2	2.1987E-06	1.7318E-05	8.3162E-05	3.3918E-04	1.9334E-05
4.4	2.1986E-06	3.0719E-05	8.3851E-05	3.4462E-04	1.9334E-05
4.6	2.1985E-06	4.4119E-05	8.4730E-05	3.5011E-04	1.9334E-05
4.8	2.1985E-06	5.7520E-05	8.5852E-05	3.5567E-04	1.9334E-05
5	2.1985E-06	7.0921E-05	8.7284E-05	3.6129E-04	1.9334E-05
5.2	2.1985E-06	8.4322E-05	8.9110E-05	3.6697E-04	1.9334E-05
5.4	2.1985E-06	9.7724E-05	9.1441E-05	3.7273E-04	1.9334E-05
5.6	2.1985E-06	1.1113E-04	9.4415E-05	3.7855E-04	1.9334E-05
5.8	2.1985E-06	1.2453E-04	9.8210E-05	3.8444E-04	1.9334E-05
6	2.1984E-06	1.3793E-04	1.0305E-04	3.9040E-04	1.9334E-05

The values of performance metrics for 100 runs are plotted in Figure(18c). The minimum, mean and maximum values of the performance metrics and fitness function are presented

TABLE 19. Analysis of the values of performance metrics obtained by ANN-BHCS algorithm for case 4.

Metrics	Best	Mean	Worst
Fitness	3.6299E-08	2.5424E-02	4.4576E-01
MAD	4.0023E-05	2.7985E-03	3.2145E-02
TIC	3.1654E-05	1.4961E-03	1.2804E-02
ENSE	1.6802E-08	4.5937E-04	1.0838E-02

TABLE 20. Convergence analysis of performance metrics for case 4.

Metrics	≤E-03	≤E-04	≤E-05	≤E-06
Fitness	81	77	69	51
MAD	91	73	24	0
TIC	94	80	54	0
ENSE	99	91	80	72

in Table(24) and plotted in Figure(18d). The convergence of fitness values and performance metrics is given in Table (25).

Histograms and box plots of fitness values and the performance metrics are given in Figure(19). Histogram of the fitness values shows that more than 80% of the values are less than equal to $E-03$ and the box plot shows that more than 75% of the values are in the range $E-04$ to $E-08$. Histogram of the MAD values shows that 90% of the values are less than or equal to $E-03$ and the box plot shows that more than 75% of the values are in the range $E-04$ to $E-05$.

TABLE 21. Statistical analysis of absolute errors for case 4 obtained by ANN-BHCS algorithm.

T	Min	Mean	SD
0	7.2404E-07	4.1534E-02	9.2749E-02
0.2	5.7474E-04	7.0811E-03	1.3970E-02
0.4	5.7435E-06	3.1909E-03	6.6080E-03
0.6	1.0761E-06	2.2074E-03	4.7458E-03
0.8	6.1497E-07	2.0732E-03	6.8365E-03
1	2.5962E-06	1.9367E-03	7.3607E-03
1.2	3.8181E-07	1.8566E-03	6.9589E-03
1.4	6.2855E-07	1.7669E-03	6.1683E-03
1.6	1.1356E-06	1.6403E-03	5.3530E-03
1.8	1.7599E-06	1.5122E-03	4.6497E-03
2	1.3967E-06	1.4128E-03	4.0860E-03
2.2	2.1928E-06	1.3306E-03	3.6568E-03
2.4	2.0680E-06	1.2721E-03	3.3342E-03
2.6	8.6171E-08	1.2355E-03	3.0904E-03
2.8	2.2005E-06	1.2016E-03	2.9086E-03
3	6.1332E-07	1.1688E-03	2.7706E-03
3.2	8.7826E-07	1.1376E-03	2.6627E-03
3.4	2.0631E-06	1.1060E-03	2.5764E-03
3.6	1.7524E-08	1.0758E-03	2.5045E-03
3.8	1.4271E-06	1.0503E-03	2.4412E-03
4	1.0384E-06	1.0230E-03	2.3863E-03
4.2	6.7506E-07	9.9280E-04	2.3383E-03
4.4	3.8338E-07	9.5935E-04	2.2964E-03
4.6	1.0838E-07	9.2335E-04	2.2603E-03
4.8	1.3665E-07	8.9032E-04	2.2281E-03
5	3.3577E-07	8.5645E-04	2.2022E-03
5.2	5.4952E-07	8.4726E-04	2.1741E-03
5.4	7.2285E-07	8.5366E-04	2.1513E-03
5.6	3.9351E-07	8.6596E-04	2.1400E-03
5.8	1.0149E-06	8.6951E-04	2.1455E-03
6	1.0071E-06	8.7980E-04	2.1705E-03

Histogram of the TIC values shows that more than 90% of the values are less than or equal to $E-03$ and the box plot shows that more than 75% of the values are in the range $E-04$ to $E-05$. Histogram of the ENSE values shows that more than 90% of the values are less than or equal to $E-03$ and the box plot shows that more than 75% of the values are in the range $E-06$ to $E-08$. The above results show the efficiency of the ANN-BHCS algorithm.

The fitness value obtained for this case is $5.2611E-08$. The convergence of the fitness values for 100 runs is given in Figure(18a). Weights obtained to minimize the fitness function are given in Figure(17a). Using these weights, the series solution for this case is given as:

$$
\begin{aligned}
\hat{\varphi}(T) = &\frac{0.0944387653654115}{1+e^{-(29.9999930359892*T-1.89439684362986)}} \\
&+\frac{3.00976959342783}{1+e^{-(-29.9999998500594*T-0.769331225730282)}} \\
&+\frac{-29.8723984892588}{1+e^{-(-7.32837775738196*T-7.21221775032898)}} \\
&+\frac{-4.72767344027581}{1+e^{-(-11.1814585234989*T-4.31578085824944)}} \\
&+\frac{29.7552610828313}{1+e^{-(-5.43107925429143*T-11.0937414279027)}} \\
&+\frac{-29.0433505482661}{1+e^{-(11.1272322542250*T+4.63641198018530)}} \\
&+\frac{29.9876754411338}{1+e^{-(-2.22947154696830*T-13.8761962234223)}} \\
&+\frac{1.13677814834999}{1+e^{-(-1.54448737763300*T-30)}} \\
&+\frac{29.7489125361151}{1+e^{-(29.9971997938506*T+2.94071451889482)}} \\
&+\frac{-1.25819303067212}{1+e^{-(-11.0879568238844*T-0.863848577605494)}}. \qquad (51)
\end{aligned}
$$

VII. COMPUTATIONAL COMPLEXITY

We have solved the first case of the problem for different number of neurons and population sizes to analyze the sensitivity of the ANN-BHCS algorithm. First, we have taken the number of neurons as 3, 5, and 10 and population size 50 which is fixed. The solutions for different number of neurons are presented in Table (27) and Figure (20a). Absolute errors for different number of neurons are given in Table (28) and Figure (20b). These results show that when the number of neurons goes form 3 to 10, the solution is getting more accurate. Now we have taken 10 neurons which is fixed and the population size is varied from 20 to 50. Solutions for different population sizes are presented in Table (29) and Figure (21a). The absolute errors for different population sizes are given in Table (30) and Figure (21b). The results show that the solution is getting better as the population size increases.

VIII. CONCLUSION

We have used a hybrid of biogeography based heterogeneous cuckoo search algorithm and artificial neural networks to solve ODEs that model the particles' velocity in a radial direction in reverse circulation air drilling. The results obtained by the ANN-BHCS algorithm are compared with the analytical results given in [24] and other algorithms. We have considered five cases of the problem based on the different values of β and μ_r. The ANN-BHCS algorithm's efficiency is checked by calculating the absolute errors, MAD, TIC, and ENSE, for five cases. The analytical solutions, which are in terms of log-sigmoid function for all the cases, are given in Eqs.(39,42,45,48) and (51). Comparison of

numerical solutions for the five cases is given in Tables. (2,7,12,17) and (22). Absolute errors for all the cases are given in Tables (3,8,13,18) and (23). The absolute errors of ANN-BHCS algorithm are from $E-03$ to $E-07$ for case 1, from $E-05$ to $E-07$ for case 2, from $E-06$ to $E-09$ for case 3, from $E-04$ to $E-06$ for case 4 and from $E-03$ to $E-07$ which shows the accuracy of the solutions obtained by the ANN-BHCS algorithm. The accuracy of the results can also be seen from the good agreement of the ANN-BHCS algorithm solutions with analytical solutions which are given in Figs. (5b,8b,11b,14b) and (17b). The efficiency of the ANN-BHCS algorithm is obvious from convergence analysis of values of performance metrics which are given in Tables (5,10,15,20,25) and Figs. (7,10,13,16) and (19). The results show that the algorithm can efficiently

TABLE 22. Solutions obtained for case 5.

T	Exact	ANN-BHCS	GA	PSO	Bat algorithm	MVO
0	0.0000000	0.0000094	-0.0001917	-0.0001466	-0.0233084	0.0405382
0.2	0.7603316	0.7615385	0.7985791	0.9573923	0.9947957	0.7984172
0.4	0.7950555	0.7951923	0.7994001	0.8303078	0.8196090	0.8004894
0.6	0.7993379	0.7993480	0.7993999	0.8044335	0.8022176	0.8004976
0.8	0.7999105	0.7999043	0.7994045	0.8005522	0.9070564	0.8004986
1	0.7999879	0.7999865	0.7998912	0.7999941	0.2840230	0.8004991
1.2	0.7999984	0.7999995	0.7998999	0.7999137	0.8012509	0.8004995
1.4	0.7999998	0.8000014	0.7999000	0.7999020	0.8028314	0.8004997
1.6	0.8000000	0.8000014	0.7999000	0.7999003	0.7955664	0.8004998
1.8	0.8000000	0.8000012	0.7999000	0.7999000	0.7875641	0.8004999
2	0.8000000	0.8000011	0.7999000	0.7999000	0.8197143	0.8004999
2.2	0.8000000	0.8000010	0.7999000	0.7999000	0.8039702	0.8005000
2.4	0.8000000	0.8000009	0.7999000	0.7999000	0.7999998	0.8005000
2.6	0.8000000	0.8000008	0.7999000	0.7999000	0.7995473	0.8005000
2.8	0.8000000	0.8000008	0.7999000	0.7999000	0.7995041	0.8005000
3	0.8000000	0.8000008	0.7999000	0.7999000	0.7995003	0.8005000
3.2	0.8000000	0.8000008	0.7999000	0.7999000	0.7995000	0.8005000
3.4	0.8000000	0.8000008	0.7999000	0.7999000	0.7995000	0.8005000
3.6	0.8000000	0.8000008	0.7999000	0.7999000	0.7995000	0.8005000
3.8	0.8000000	0.8000008	0.7999000	0.7999000	0.7995000	0.8005000
4	0.8000000	0.8000008	0.7999000	0.7999000	0.7995000	0.8005000
4.2	0.8000000	0.8000008	0.7999000	0.7999000	0.7995000	0.8005000
4.4	0.8000000	0.8000008	0.7999000	0.7999000	0.7995000	0.8005000
4.6	0.8000000	0.8000008	0.7999000	0.7999000	0.7995000	0.8005000
4.8	0.8000000	0.8000008	0.7999000	0.7999000	0.7995000	0.8005000
5	0.8000000	0.8000008	0.7999000	0.7999000	0.7995000	0.8005000
5.2	0.8000000	0.8000008	0.7999000	0.7999000	0.7995000	0.8005000
5.4	0.8000000	0.8000008	0.7999000	0.7999000	0.7995000	0.8005000
5.6	0.8000000	0.8000008	0.7999000	0.7999000	0.7995000	0.8005000
5.8	0.8000000	0.8000008	0.7999000	0.7999000	0.7995000	0.8005000
6	0.8000000	0.8000008	0.7999000	0.7999000	0.7995000	0.8005000

TABLE 23. Comparison of absolute errors of BHCS and other algorithms for case 5.

T	ANN-BHCS	GA	PSO	Bat algorithm	MVO
0	9.3971E-06	1.9175E-04	1.4664E-04	2.3308E-02	4.0538E-02
0.2	1.2070E-03	3.8247E-02	1.9706E-01	2.3446E-01	3.8086E-02
0.4	1.3681E-04	4.3447E-03	3.5252E-02	2.4554E-02	5.4339E-03
0.6	1.0061E-05	6.1975E-05	5.0956E-03	2.8797E-03	1.1597E-03
0.8	6.2203E-06	5.0599E-04	6.4170E-04	1.0715E-01	5.8806E-04
1	1.4410E-06	9.6665E-05	6.1642E-06	5.1596E-01	5.1124E-04
1.2	1.1336E-06	9.8415E-05	8.4671E-05	1.2525E-03	5.0111E-04
1.4	1.6159E-06	9.9821E-05	9.7771E-05	2.8317E-03	4.9989E-04
1.6	1.4718E-06	1.0000E-04	9.9673E-05	4.4336E-03	4.9983E-04
1.8	1.2514E-06	1.0002E-04	9.9956E-05	1.2436E-02	4.9988E-04
2	1.0795E-06	1.0002E-04	9.9993E-05	1.9714E-02	4.9993E-04
2.2	9.6316E-07	1.0001E-04	9.9999E-05	3.9702E-03	4.9995E-04
2.4	8.8761E-07	1.0001E-04	1.0000E-04	1.5582E-07	4.9997E-04
2.6	8.3916E-07	1.0001E-04	1.0000E-04	4.5268E-04	4.9998E-04
2.8	8.0819E-07	1.0001E-04	1.0000E-04	4.9585E-04	4.9999E-04
3	7.8839E-07	1.0000E-04	1.0000E-04	4.9965E-04	4.9999E-04
3.2	7.7573E-07	1.0000E-04	1.0000E-04	4.9997E-04	5.0000E-04
3.4	7.6762E-07	1.0000E-04	1.0000E-04	5.0000E-04	5.0000E-04
3.6	7.6244E-07	1.0000E-04	1.0000E-04	5.0000E-04	5.0000E-04
3.8	7.5912E-07	1.0000E-04	1.0000E-04	5.0000E-04	5.0000E-04
4	7.5700E-07	1.0000E-04	1.0000E-04	5.0000E-04	5.0000E-04
4.2	7.5564E-07	1.0000E-04	1.0000E-04	5.0000E-04	5.0000E-04
4.4	7.5476E-07	1.0000E-04	1.0000E-04	5.0000E-04	5.0000E-04
4.6	7.5421E-07	1.0000E-04	1.0000E-04	5.0000E-04	5.0000E-04
4.8	7.5385E-07	1.0000E-04	1.0000E-04	5.0000E-04	5.0000E-04
5	7.5362E-07	1.0000E-04	1.0000E-04	5.0000E-04	5.0000E-04
5.2	7.5347E-07	1.0000E-04	1.0000E-04	5.0000E-04	5.0000E-04
5.4	7.5338E-07	1.0000E-04	1.0000E-04	5.0000E-04	5.0000E-04
5.6	7.5332E-07	1.0000E-04	1.0000E-04	5.0000E-04	5.0000E-04
5.8	7.5328E-07	1.0000E-04	1.0000E-04	5.0000E-04	5.0000E-04
6	7.5326E-07	1.0000E-04	1.0000E-04	5.0000E-04	5.0000E-04

minimize the fitness function and obtains the best solution as more than 90% values of the fitness function and performance metrics are less than $E-03$.

TABLE 24. Minimum, mean and maximum values of performance metrics obtained by ANN-BHCS algorithm for case 5.

Metrics	Best	Mean	Worst
Fitness	2.9722E-08	3.6813E-02	7.4670E-01
MAD	3.7939E-05	6.0162E-03	3.4170E-01
TIC	2.8194E-05	2.1714E-03	5.2392E-02
ENSE	1.6818E-08	1.4244E-02	3.6418E-01

TABLE 25. Convergence analysis of performance metrics for case 5.

Metrics	≤E-03	≤E-04	≤E-05	≤E-06
Fitness	83	81	76	61
MAD	89	80	38	0
TIC	92	82	69	0
ENSE	97	89	82	80

NOMENCLATURE

d_{sv} Diameter of the particle.
V_s Volume of the particle.
F_d Aerodynamic drag force.
C_D Drag coefficient.
A_r Projected area of the particle.
ρ_g Density of air.
v_g Velocity of air.
v_s Velocity of particle.
G_s Weight of the particle.
m_s Mass of the particle.

TABLE 26. Statistical analysis of absolute errors for case 5 obtained by ANN-BHCS algorithm.

T	Min	Mean	SD
0	4.0589E-07	4.4548E-02	1.2934E-01
0.2	3.8138E-04	5.5382E-03	1.1116E-02
0.4	1.6277E-05	3.8300E-03	1.0912E-02
0.6	6.5828E-07	3.5285E-03	1.0803E-02
0.8	1.4448E-06	3.9947E-03	2.0396E-02
1	7.2521E-07	4.6888E-03	3.4715E-02
1.2	9.7928E-07	4.8710E-03	3.9112E-02
1.4	5.1705E-07	4.8885E-03	3.9939E-02
1.6	3.2429E-07	4.8276E-03	4.0057E-02
1.8	1.4943E-07	4.7785E-03	4.0056E-02
2	5.1116E-07	4.7421E-03	4.0041E-02
2.2	9.6316E-07	4.7007E-03	4.0030E-02
2.4	8.8761E-07	4.6585E-03	4.0025E-02
2.6	8.3916E-07	4.6137E-03	4.0024E-02
2.8	3.3674E-07	4.6230E-03	4.0020E-02
3	7.8839E-07	4.6329E-03	4.0020E-02
3.2	7.7573E-07	4.6425E-03	4.0022E-02
3.4	5.5349E-08	4.6586E-03	4.0026E-02
3.6	7.1575E-07	4.6891E-03	4.0030E-02
3.8	2.6269E-07	4.7192E-03	4.0037E-02
4	1.8256E-07	4.7502E-03	4.0045E-02
4.2	6.1526E-07	4.7888E-03	4.0055E-02
4.4	6.9474E-07	4.8289E-03	4.0067E-02
4.6	7.5421E-07	4.8689E-03	4.0081E-02
4.8	4.1544E-07	4.9092E-03	4.0097E-02
5	6.2220E-08	4.9505E-03	4.0114E-02
5.2	4.1260E-07	4.9889E-03	4.0134E-02
5.4	7.5338E-07	5.0205E-03	4.0157E-02
5.6	7.5332E-07	5.0402E-03	4.0183E-02
5.8	6.7018E-09	5.0653E-03	4.0209E-02
6	7.5326E-07	5.1185E-03	4.0238E-02

TABLE 27. Solutions obtained by ANN-BHCS algorithm for different number of neurons.

T	Analytical	3 neurons	5 neurons	10 neurons
0	0.00000000	0.0000160	0.0000052	0.0005401
0.2	0.81770000	0.9123153	0.9151193	0.8204161
0.4	0.88150760	0.9106588	0.9110115	0.8817631
0.6	0.89972090	0.9105721	0.9106924	0.9000188
0.8	0.90628010	0.9105696	0.9106740	0.9064060
1	0.90883300	0.9105695	0.9106658	0.9088077
1.2	0.90985630	0.9105695	0.9106578	0.9097774
1.4	0.91027140	0.9105695	0.9106499	0.9101944
1.6	0.91044050	0.9105695	0.9106420	0.9103831
1.8	0.91050960	0.9105695	0.9106341	0.9104717
2	0.91053780	0.9105695	0.9106261	0.9105145
2.2	0.91054930	0.9105695	0.9106182	0.9105356
2.4	0.91055400	0.9105695	0.9106103	0.9105461
2.6	0.91055590	0.9105695	0.9106025	0.9105514
2.8	0.91055670	0.9105695	0.9105946	0.9105540
3	0.91055710	0.9105695	0.9105869	0.9105553
3.2	0.91055720	0.9105695	0.9105792	0.9105560
3.4	0.91055720	0.9105695	0.9105715	0.9105563
3.6	0.91055730	0.9105695	0.9105641	0.9105565
3.8	0.91055730	0.9105695	0.9105569	0.9105565
4	0.91055730	0.9105695	0.9105499	0.9105566
4.2	0.91055730	0.9105695	0.9105433	0.9105566
4.4	0.91055730	0.9105695	0.9105373	0.9105566
4.6	0.91055730	0.9105695	0.9105321	0.9105566
4.8	0.91055730	0.9105695	0.9105279	0.9105566
5	0.91055730	0.9105695	0.9105252	0.9105566
5.2	0.91055730	0.9105695	0.9105245	0.9105566
5.4	0.91055730	0.9105695	0.9105267	0.9105566
5.6	0.91055730	0.9105695	0.9105326	0.9105566
5.8	0.91055730	0.9105695	0.9105439	0.9105566
6	0.91055730	0.9105695	0.9105625	0.9105566

TABLE 28. Absolute errors for different number of neurons.

T	3 neurons	5 neurons	10 neurons
0	1.6092E-05	5.2123E-06	5.4012E-04
0.2	9.4615E-02	9.7419E-02	2.7161E-03
0.4	2.9151E-02	2.9504E-02	2.5551E-04
0.6	1.0851E-02	1.0972E-02	2.9796E-04
0.8	4.2896E-03	4.3939E-03	1.2589E-04
1	1.7366E-03	1.8328E-03	2.5267E-05
1.2	7.1325E-04	8.0155E-04	7.8899E-05
1.4	2.9820E-04	3.7857E-04	7.6948E-05
1.6	1.2906E-04	2.0150E-04	5.7434E-05
1.8	6.0002E-05	1.2452E-04	3.7828E-05
2	3.1783E-05	8.8378E-05	2.3222E-05
2.2	2.0248E-05	6.8934E-05	1.3683E-05
2.4	1.5533E-05	5.6324E-05	7.9041E-06
2.6	1.3605E-05	4.6526E-05	4.5726E-06
2.8	1.2817E-05	3.7904E-05	2.7204E-06
3	1.2495E-05	2.9800E-05	1.7204E-06
3.2	1.2363E-05	2.1961E-05	1.1946E-06
3.4	1.2309E-05	1.4306E-05	9.2542E-07
3.6	1.2287E-05	6.8319E-06	7.9163E-07
3.8	1.2278E-05	4.2207E-07	7.2756E-07
4	1.2274E-05	7.3820E-06	6.9842E-07
4.2	1.2273E-05	1.3939E-05	6.8622E-07
4.4	1.2272E-05	1.9940E-05	6.8186E-07
4.6	1.2272E-05	2.5173E-05	6.8091E-07
4.8	1.2272E-05	2.9344E-05	6.8125E-07
5	1.2272E-05	3.2049E-05	6.8197E-07
5.2	1.2272E-05	3.2731E-05	6.8268E-07
5.4	1.2272E-05	3.0620E-05	6.8326E-07
5.6	1.2272E-05	2.4658E-05	6.8369E-07
5.8	1.2272E-05	1.3381E-05	6.8399E-07
6	1.2272E-05	5.2229E-06	6.8420E-07

TABLE 29. Solutions obtained by ANN-BHCS algorithm for different population sizes.

T	Analytical	Pop=20	Pop=30	Pop=50
0	0	0.0031725	0.0000139	0.0005401
0.2	0.8177	1.0546045	0.9275984	0.8204161
0.4	0.881508	1.0173661	0.9169540	0.8817631
0.6	0.899721	0.9770457	0.9133947	0.9000188
0.8	0.90628	0.9468821	0.9117944	0.906406
1	0.908833	0.9287682	0.9110267	0.9088077
1.2	0.909856	0.9188651	0.9106635	0.9097774
1.4	0.910271	0.9137513	0.9105026	0.9101944
1.6	0.91044	0.9112617	0.9104428	0.9103831
1.8	0.91051	0.9101558	0.9104324	0.9104717
2	0.910538	0.9097523	0.9104444	0.9105145
2.2	0.910549	0.9096870	0.9104651	0.9105356
2.4	0.910554	0.9097700	0.9104877	0.9105461
2.6	0.910556	0.9099058	0.9105090	0.9105514
2.8	0.910557	0.9100490	0.9105277	0.910554
3	0.910557	0.9101798	0.9105434	0.9105553
3.2	0.910557	0.9102915	0.9105563	0.910556
3.4	0.910557	0.9103835	0.9105668	0.9105563
3.6	0.910557	0.9104575	0.9105751	0.9105565
3.8	0.910557	0.9105165	0.9105818	0.9105565
4	0.910557	0.9105632	0.9105870	0.9105566
4.2	0.910557	0.9106000	0.9105912	0.9105566
4.4	0.910557	0.9106292	0.9105944	0.9105566
4.6	0.910557	0.9106524	0.9105969	0.9105566
4.8	0.910557	0.9106710	0.9105989	0.9105566
5	0.910557	0.9106860	0.9106005	0.9105566
5.2	0.910557	0.9106985	0.9106017	0.9105566
5.4	0.910557	0.9107090	0.9106026	0.9105566
5.6	0.910557	0.9107181	0.9106034	0.9105566
5.8	0.910557	0.9107264	0.9106040	0.9105566
6	0.910557	0.9107342	0.9106044	0.9105566

TABLE 30. Absolute errors for different population sizes.

T	Pop=20	Pop=30	Pop=50
0	3.1725E-03	1.3904E-05	5.4012E-04
0.2	2.3690E-01	1.0990E-01	2.7161E-03
0.4	1.3586E-01	3.5446E-02	2.5551E-04
0.6	7.7325E-02	1.3674E-02	2.9796E-04
0.8	4.0602E-02	5.5143E-03	1.2589E-04
1	1.9935E-02	2.1937E-03	2.5267E-05
1.2	9.0088E-03	8.0723E-04	7.8899E-05
1.4	3.4800E-03	2.3124E-04	7.6948E-05
1.6	8.2118E-04	2.3277E-06	5.7434E-05
1.8	3.5380E-04	7.7181E-05	3.7828E-05
2	7.8547E-04	9.3367E-05	2.3222E-05
2.2	8.6234E-04	8.4160E-05	1.3683E-05
2.4	7.8404E-04	6.6276E-05	7.9041E-06
2.6	6.5012E-04	4.6937E-05	4.5726E-06
2.8	5.0774E-04	2.9074E-05	2.7204E-06
3	3.7724E-04	1.3677E-05	1.7204E-06
3.2	2.6566E-04	8.8447E-07	1.1946E-06
3.4	1.7378E-04	9.5179E-06	9.2542E-07
3.6	9.9737E-05	1.7864E-05	7.9163E-07
3.8	4.0783E-05	2.4500E-05	7.2756E-07
4	5.8731E-06	2.9747E-05	6.9842E-07
4.2	4.2731E-05	3.3877E-05	6.8622E-07
4.4	7.1897E-05	3.7119E-05	6.8186E-07
4.6	9.5088E-05	3.9660E-05	6.8091E-07
4.8	1.1368E-04	4.1647E-05	6.8125E-07
5	1.2876E-04	4.3200E-05	6.8197E-07
5.2	1.4121E-04	4.4412E-05	6.8268E-07
5.4	1.5171E-04	4.5358E-05	6.8326E-07
5.6	1.6085E-04	4.6097E-05	6.8369E-07
5.8	1.6911E-04	4.6672E-05	6.8399E-07
6	1.7689E-04	4.7121E-05	6.8420E-07

ρ_s Density of the particle.
g Gravitational acceleration.
f_r Frictional force.
μ_r Coefficient of friction.
d_{cd} Critical diameter of the particle.
v_{cv} Critical velocity of the particle.
f Activation function.
j Total number of neurons.
$\alpha_i, \beta_i, \omega_i$ Unknown weights.
$\hat{\varphi}(T)$ Approximate series solution.
E_1 Solution error of ordinary differential equation.
E_2 Solution error of initial/boundary values.
ANNs Artificial Neural Networks.
ODE Ordinary Differential Equation.
BBO Biogeography based optimization.
CS Cuckoo search.
BHCS Biogeography based heterogeneous cuckoo search.
TS Tabu search.
GA Genetic algorithm.
PSO Particle swarm optimization.
MVO Multiverse optimizer.
HA Hybrid algorithms.
MA Modified algorithms.
IWD Intelligent water drop.
SI Swarm intelligent.
AI Artificial intelligence.
FF Firefly.
MOA Magnetic optimization algorithm.
FL Frog leaping.
SO Single objective.
MO Multiobjective.
TIC Theil's Inequality Coefficient.
MAD Mean Absolute Deviation.
NSE Nash–Sutcliffe Efficiency.
ENSE Error in Nash–Sutcliffe efficiency.

REFERENCES

[1] R. R. Angel, "Volume requirements for air or gas drilling," *Trans. AIME*, vol. 210, no. 01, pp. 325–330, Dec. 1957.
[2] B. Guo and A. Ghalambor, *Gas Volume Requirements for Underbalanced Drilling: Deviated Holes*. Tulsa, Oklahoma: PennWell Books, 2002.
[3] A. Grant and A. D. Briggs, "Toxicity of sediments from around a North Sea oil platform: Are metals or hydrocarbons responsible for ecological impacts?" *Mar. Environ. Res.*, vol. 53, no. 1, pp. 95–116, Feb. 2002.
[4] M. S. Kalsi, P. D. Alvarez, D. Somogyi, and A. Richie, "Load-responsive hydrodynamic bearing for downhole drilling tools," *ASME. J. Tribol.*, vol. 129, no. 1, pp. 209–217, Jan. 2007, doi: 10.1115/1.2404963.
[5] A. N. Khondaker, "Modeling the fate of drilling waste in Marine environment—An overview," *Comput. Geosci.*, vol. 26, no. 5, pp. 531–540, Jun. 2000.
[6] O.-Y. Yu, Z. Medina-Cetina, S. D. Guikema, J.-L. Briaud, and D. Burnett, "Integrated approach for the optimal selection of environmentally friendly drilling systems," *Int. J. Energy Environ. Eng.*, vol. 3, no. 1, p. 25, 2012.
[7] C. L. William, B. Guo, and A. Frank, *Air and Gas Drilling Manual*. New York, NY, USA: McGraw-Hill, 2001.
[8] H.-J. Henzler, "Design of ejectors for single-phase material systems," *Chem. Ingenieur Technik*, vol. 54, no. 1, pp. 8–16, 1982.
[9] W. Lyons, B. Guo, and F. Seidel, "Air and gas drilling manual. Translated by Zeng Yi-jin, Fan Hong-Hai," China Petrochemical Press, Beijing, China, 2006.
[10] H.-S. Shan and G.-Q. Yao, "Nontraditional reservoir and oil resources sustainable development," *Special Oil Gas Reservoirs*, vol. 3, 2004.
[11] H. Rye, M. Reed, and N. Ekrol, "The PARTRACK model for calculation of the spreading and deposition of drilling mud, chemicals and drill cuttings," *Environ. Model. Softw.*, vol. 13, nos. 5–6, pp. 431–441, Oct. 1998.
[12] M. T. Schaanning, H. C. Trannum, S. Øxnevad, J. Carroll, and T. Bakke, "Effects of drill cuttings on biogeochemical fluxes and macrobenthos of Marine sediments," *J. Experim. Mar. Biol. Ecol.*, vol. 361, no. 1, pp. 49–57, Jun. 2008.
[13] I. Singsaas, H. Rye, T. K. Frost, M. G. Smit, E. Garpestad, I. Skare, K. Bakke, L. F. Veiga, M. Buffagni, O. A. Folium, and S. Johnsen, "Development of a risk-based environmental management tool for drilling discharges. summary of a four-year project," *Integr. Environ. Assessment Manage.*, vol. 4, no. 2, pp. 171–176, 2008.
[14] J. Deng, L. Zou, Q. Tan, W. Yan, D. Gao, H. Zhang, and X. Yan, "Critical condition study of borehole stability during air drilling," *Petroleum Sci.*, vol. 6, no. 2, pp. 158–165, Jun. 2009.
[15] O. Cazarez-Candia and M. A. Vásquez-Cruz, "Prediction of pressure, temperature, and velocity distribution of two-phase flow in oil wells," *J. Petroleum Sci. Eng.*, vol. 46, no. 3, pp. 195–208, Mar. 2005.
[16] N. K. Korsakova and V. I. Pen'kovskii, "Phase distribution and intrapore salt exchange during drilling mud invasion of an oil- and gas-bearing formation," *Fluid Dyn.*, vol. 44, no. 2, pp. 270–277, Apr. 2009.
[17] H. Rye, M. Reed, T. K. Frost, and T. I. Røe Utvik, "Comparison of the ParTrack mud/cuttings release model with field data," *Environ. Model. Softw.*, vol. 19, nos. 7–8, pp. 701–716, Jul. 2004.
[18] Z. Wang and B. Sun, "Annular multiphase flow behavior during deep water drilling and the effect of hydrate phase transition," *Petroleum Sci.*, vol. 6, no. 1, pp. 57–63, Mar. 2009.
[19] V. A. Yasashin, N. G. Makarov, A. M. Nazarov, and D. Y. Serikov, "New design of drilling bit with centrifugally through-hardened cutter structure, for jetturbine drilling," *Chem. Petroleum Eng.*, vol. 32, no. 2, pp. 115–118, Mar. 1996.
[20] S. R. Bhutada and V. G. Pangarkar, "Gas induction and hold-up characteristics of liquid jet loop reactors," *Chem. Eng. Commun.*, vol. 61, nos. 1–6, pp. 239–258, Nov. 1987.
[21] Y. B. Nakhi and S. L. Kalla, "Some boundary value problems of temperature fields in oil strata," *Appl. Math. Comput.*, vol. 146, no. 1, pp. 105–119, Dec. 2003.

[22] S. Pelipenko and I. A. Frigaard, "Mud removal and cement placement during primary cementing of an oil well—Part 2; steady-state displacements," *J. Eng. Math.*, vol. 48, no. 1, pp. 1–26, Jan. 2004.

[23] Z. Li and B. Guo, "Analysis of longitudinal vibration of drill string in air and gas drilling," presented at the Rocky Mountain Oil Gas Technol. Symp., Denver, CO, USA, Apr. 2007, doi: 10.2118/107697-MS.

[24] L. H. Zhu, Y. Huang, R. H. Wang, and J. Y. Wang, "A mathematical model of the motion of cutting particles in reverse circulation air drilling," *Appl. Math. Comput.*, vol. 256, pp. 192–202, Apr. 2015.

[25] J. Liu, *Researches on the Key Technologies of Hollow-Through DTH Used in Gas Drilling*. Changchun, China: Jilin Univ., 2009.

[26] Y. Zhu, W. Cai, C. Wen, and Y. Li, "Numerical investigation of geometry parameters for design of high performance ejectors," *Appl. Thermal Eng.*, vol. 29, nos. 5–6, pp. 898–905, 2009.

[27] W. Huang, T. Jiang, X. Zhang, N. A. Khan, and M. Sulaiman, "Analysis of beam-column designs by varying axial load with internal forces and bending rigidity using a new soft computing technique," *Complexity*, vol. 2021, pp. 1–19, Mar. 2021.

[28] Y. Zhang, J. Lin, Z. Hu, N. A. Khan, and M. Sulaiman, "Analysis of third-order nonlinear multi-singular Emden-Fowler equation by using the LeNN-WOA-NM algorithm," *IEEE Access*, vol. 9, pp. 72111–72138, 2021.

[29] N. A. Khan, M. Sulaiman, P. Kumam, and A. J. Aljohani, "A new soft computing approach for studying the wire coating dynamics with Oldroyd 8-constant fluid," *Phys. Fluids*, vol. 33, no. 3, Mar. 2021, Art. no. 036117.

[30] A. Ahmad, M. Sulaiman, A. J. Aljohani, A. Alhindi, and H. Alrabaiah, "Design of an efficient algorithm for solution of Bratu differential equations," *Ain Shams Eng. J.*, vol. 12, no. 2, pp. 2211–2225, Jun. 2021.

[31] A. Ahmad, M. Sulaiman, A. Alhindi, and A. J. Aljohani, "Analysis of temperature profiles in longitudinal fin designs by a novel neuroevolutionary approach," *IEEE Access*, vol. 8, pp. 113285–113308, 2020.

[32] M. Sulaiman, M. Sulaman, A. Hamdi, and Z. Hussain, "The plant propagation algorithm for the optimal operation of directional over-current relays in electrical engineering," *Mehran Univ. Res. J. Eng. Technol.*, vol. 39, no. 2, pp. 223–236, Apr. 2020.

[33] W. Waseem, M. Sulaiman, S. Islam, P. Kumam, R. Nawaz, M. A. Z. Raja, M. Farooq, and M. Shoaib, "A study of changes in temperature profile of porous fin model using cuckoo search algorithm," *Alexandria Eng. J.*, vol. 59, no. 1, pp. 11–24, 2020.

[34] A. H. Bukhari, M. Sulaiman, S. Islam, M. Shoaib, P. Kumam, and M. A. Z. Rajaf, "Neuro-fuzzy modeling and prediction of summer precipitation with application to different meteorological stations," *Alexandria Eng. J.*, vol. 59, no. 1, pp. 101–116, 2020.

[35] A. H. Bukhari, M. A. Z. Raja, M. Sulaiman, S. Islam, M. Shoaib, and P. Kumam, "Fractional neuro-sequential ARFIMA-LSTM for financial market forecasting," *IEEE Access*, vol. 8, pp. 71326–71338, 2020.

[36] W. Waseem, M. Sulaiman, A. Alhindi, and H. Alhakami, "A soft computing approach based on fractional order DPSO algorithm designed to solve the corneal model for eye surgery," *IEEE Access*, vol. 8, pp. 61576–61592, 2020.

[37] A. H. Bukhari, M. Sulaiman, M. A. Z. Raja, S. Islam, M. Shoaib, and P. Kumam, "Design of a hybrid NAR-RBFs neural network for nonlinear dusty plasma system," *Alexandria Eng. J.*, vol. 59, no. 5, pp. 3325–3345, Oct. 2020.

[38] A. Khan, M. Sulaiman, H. Alhakami, and A. Alhindi, "Analysis of oscillatory behavior of heart by using a novel neuroevolutionary approach," *IEEE Access*, vol. 8, pp. 86674–86695, 2020.

[39] W. Waseem, M. Sulaiman, P. Kumam, M. Shoaib, M. A. Z. Raja, and S. Islam, "Investigation of singular ordinary differential equations by a neuroevolutionary approach," *PLoS ONE*, vol. 15, no. 7, Jul. 2020, Art. no. e0235829.

[40] W. Waseem, M. Sulaiman, and A. J. Aljohani, "Investigation of fractional models of damping material by a neuroevolutionary approach," *Chaos, Solitons Fractals*, vol. 140, Nov. 2020, Art. no. 110198.

[41] S. Ahmad, M. Sulaiman, P. Kumam, Z. Hussain, M. A. Jan, W. K. Mashwani, and M. Ullah, "A novel population initialization strategy for accelerating levy flights based multi-verse optimizer," *J. Intell. Fuzzy Syst.*, vol. 39, no. 1, pp. 1–17, 2020.

[42] M. Sulaiman, S. Ahmad, J. Iqbal, A. Khan, and R. Khan, "Optimal operation of the hybrid electricity generation system using multiverse optimization algorithm," *Comput. Intell. Neurosci.*, vol. 2019, pp. 1–12, Mar. 2019.

[43] M. Sulaiman, M. Masihullah, Z. Hussain, S. Ahmad, W. K. Mashwani, M. A. Jan, and R. A. Khanum, "Implementation of improved grasshopper optimization algorithm to solve economic load dispatch problems," *Hacettepe J. Math. Statist.*, vol. 48, no. 5, pp. 1570–1589, 2019.

[44] M. Sulaiman, I. Samiullah, A. Hamdi, and Z. Hussain, "An improved whale optimization algorithm for solving multi-objective design optimization problem of PFHE," *J. Intell. Fuzzy Syst.*, vol. 37, no. 3, pp. 3815–3828, Oct. 2019.

[45] M. Sulaiman, A. Ahmad, A. Khan, and S. Muhammad, "Hybridized symbiotic organism search algorithm for the optimal operation of directional overcurrent relays," *Complexity*, vol. 2018, pp. 1–11, Jan. 2018.

[46] M. Sulaiman, Waseem, S. Muhammad, and A. Khan, "Improved solutions for the optimal coordination of DOCRs using firefly algorithm," *Complexity*, vol. 2018, pp. 1–15, Feb. 2018.

[47] B. I. Selamoğlu, A. Salhi, and M. Sulaiman, "Strip algorithms as an efficient way to initialise population-based metaheuristics," in *Recent Developments in Metaheuristics*. Cham, Switzerland: Springer, 2018, pp. 319–331.

[48] M. Sulaiman and A. Salhi, "A hybridisation of runner-based and seed-based plant propagation algorithms," in *Nature-Inspired Computation in Engineering*. Cham, Switzerland: Springer, 2016, pp. 195–215.

[49] M. Sulaiman and A. Salhi, "A seed-based plant propagation algorithm: The feeding station model," *Sci. World J.*, vol. 2015, pp. 1–16, Jan. 2015.

[50] M. Sulaiman, A. Salhi, B. I. Selamoglu, and O. B. Kirikchi, "A plant propagation algorithm for constrained engineering optimisation problems," *Math. Problems Eng.*, vol. 2014, pp. 1–10, Jan. 2014.

[51] N. S. Shahraki and S. H. Zahiri, "Multi-objective optimization algorithms in analog active filter design," in *Proc. 8th Iranian Joint Congr. Fuzzy Intell. Syst. (CFIS)*, Sep. 2020, pp. 105–109.

[52] P. Antil, S. K. Antil, C. Prakash, G. Królczyk, and C. Pruncu, "Multi-objective optimization of drilling parameters for orthopaedic implants," *Meas. Control*, vol. 53, nos. 9–10, pp. 1902–1910, Nov. 2020.

[53] A. Mohammadi, M. Mohammadi, and S. H. Zahiri, "Design of optimal CMOS ring oscillator using an intelligent optimization tool," *Soft Comput.*, vol. 22, no. 24, pp. 8151–8166, Dec. 2018.

[54] K. Wang, R. Wang, Y. Liu, and G. Song, "Multi-objective optimization of drilling parameters based on Pareto optimality," *China Mech. Eng.*, vol. 28, no. 13, p. 1580, 2017.

[55] A. Mohammadi, M. Mohammadi, and S. H. Zahiri, "A novel solution based on multi-objective ai techniques for optimization of CMOS lc_vcos," *J. Telecommun., Electron. Comput. Eng. (JTEC)*, vol. 7, no. 2, pp. 137–144, 2015.

[56] B. Chopard and M. Tomassini, *An Introduction to Metaheuristics for Optimization*. Springer, 2018.

[57] R. L. Yadav and A. W. Patwardhan, "Design aspects of ejectors: Effects of suction chamber geometry," *Chem. Eng. Sci.*, vol. 63, no. 15, pp. 3886–3897, Aug. 2008.

[58] S. Gupta, D. K. Majhi, and S. K. Vishwakarma, "Torsional surface wave propagation in an initially stressed non-homogeneous layer over a non-homogeneous half-space," *Appl. Math. Comput.*, vol. 219, no. 6, pp. 3209–3218, Nov. 2012.

[59] R. Rajabioun, "Cuckoo optimization algorithm," *Appl. Soft Comput.*, vol. 11, no. 8, pp. 5508–5518, Aug. 2011.

[60] I. Fister, Jr., X. S. Yang, D. Fister, and I. Fister, "Cuckoo search: A brief literature review," in *Cuckoo Search and Firefly Algorithm: Theory and Applications*, vol. 516. Cham, Switzerland: Springer, 2014, pp. 49–62.

[61] F. Kolahan and M. Liang, "A Tabu search approach to optimization of drilling operations," *Comput. Ind. Eng.*, vol. 31, nos. 1–2, pp. 371–374, Oct. 1996.

[62] F. Kolahan and M. Liang, "Optimization of hole-making operations: A tabu-search approach," *Int. J. Mach. Tools Manuf.*, vol. 40, no. 12, pp. 1735–1753, Sep. 2000.

[63] C. Tsai, C. Liu, and Y. Wang, "Application of genetic algorithm on ic substrate drilling path optimization," in *Proc. Int. Conf. Adv. Mech. Syst.*, Sep. 2012, pp. 441–446.

[64] A. Dalavi, P. Pawar, T. Singh, A. Warke, and P. Paliwal, "Review on optimization of hole-making operations for injection mould using non-traditional algorithms," *Int. J. Ind. Eng. Manag.*, vol. 7, no. 1, pp. 9–14, 2016.

[65] J. Zhang, "Optimization algorithm of holes machining path," in *Proc. 2nd Int. Conf. Electron. Mech. Eng. Inf. Technol.*, Paris, France: Atlantis Press, 2012, pp. 1–4.

[66] D. H. Al-Janan and T.-K. Liu, "Path optimization of CNC PCB drilling using hybrid Taguchi genetic algorithm," *Kybernetes*, vol. 45, no. 1, pp. 107–125, Jan. 2016.

[67] W. C. E. Lim, G. Kanagaraj, and S. G. Ponnambalam, "A hybrid cuckoo search-genetic algorithm for hole-making sequence optimization," *J. Intell. Manuf.*, vol. 27, no. 2, pp. 417–429, Apr. 2016.

[68] S. Mirjalili and A. Lewis, "The whale optimization algorithm," *Adv. Eng. Softw.*, vol. 95, pp. 51–67, May 2016.
[69] S. Mirjalili, "Dragonfly algorithm: A new meta-heuristic optimization technique for solving single-objective, discrete, and multi-objective problems," *Neural Comput. Appl.*, vol. 27, no. 4, pp. 1053–1073, 2016.
[70] N. Tamta and R. S. Jadoun, "Parametric optimization of drilling machining process for surface roughness on aluminium alloy 6082 using Taguchi method," *J. Mater. Environ. Sci.*, vol. 2, no. 7, pp. 49–55, 2015.
[71] H. C. Yang, K. J. Liu, and M. H. Hung, "Drill-path optimization with time limit and thermal protection," *Adv. Mater. Res.*, vol. 579, pp. 153–159, Oct. 2012.
[72] R. Poli, J. Kennedy, and T. Blackwell, "Particle swarm optimization," *Swarm Intell.*, vol. 1, no. 1, pp. 33–57, Jun. 2007.
[73] P. R. Srivastava, "A cooperative approach to optimize the printed circuit boards drill routing process using intelligent water drops," *Comput. Electr. Eng.*, vol. 43, pp. 270–277, Apr. 2015.
[74] G. Y. Zhu, "Drilling path optimization based on swarm intelligent algorithm," in *Proc. IEEE Int. Conf. Robot. Biomimetics*, Dec. 2006, pp. 193–196.
[75] H. Abdullah, R. Ramli, D. Wahab, and J. Qudeiri, "Simulation approach of cutting tool movement using artificial intelligence method," *J. Eng. Sci. Technol.*, vol. 10, no. 2014, pp. 35–44, 2015.
[76] M. M. Ismail, M. A. Othman, H. A. Sulaiman, M. H. Misran, R. H. Ramlee, A. F. Z. Abidin, N. A. Nordin, M. I. Zakaria, M. N. Ayob, and F. Yakop, "Firefly algorithm for path optimization in PCB holes drilling process," in *Proc. Int. Conf. Green Ubiquitous Technol.*, Jul. 2012, pp. 110–113.
[77] M. M. Ismail, M. A. Othman, H. A. Sulaiman, M. A. M. Said, M. H. Misran, R. A. Ramlee, M. Sinnappa, Z. Zakaria, B. H. Ahmad, A. A. MZA, and K. Osman, "Route planning analysis in holes drilling process using magnetic optimization algorithm for electronic manufacturing sector," *World Appl. Sci. J.*, vol. 21, no. 2, pp. 91–97, 2013.
[78] A. M. Dalavi, P. J. Pawar, and T. P. Singh, "Optimal sequence of hole-making operations using particle swarm optimization and modified shuffled frog leaping algorithm," *Eng. Rev., Meunarodni Časopis Namijenjen Publiciranju Originalnih Istraživanja s Aspekta Analize Konstrukcija, Materijala i Novih Tehnologija u Području Strojarstva, Brodogradnje, Temeljnih Tehničkih Znanosti, Elektrotehnike, Računarstva i Graevinarstva*, vol. 36, no. 2, pp. 187–196, 2016.
[79] A. Hassan, S.-U.-I. Ahmad, M. Kamran, A. Illahi, and R. M. A. Zahoor, "Design of cascade artificial neural networks optimized with the memetic computing paradigm for solving the nonlinear Bratu system," *Eur. Phys. J. Plus*, vol. 134, no. 3, pp. 1–13, Mar. 2019.
[80] X.-S. Yang and S. Deb, "Cuckoo search via Lévy flights," in *Proc. World Congr. Nature Biologically Inspired Comput. (NaBIC)*, Dec. 2009, pp. 210–214.
[81] X. Ding, Z. Xu, N. J. Cheung, and X. Liu, "Parameter estimation of Takagi–Sugeno fuzzy system using heterogeneous cuckoo search algorithm," *Neurocomputing*, vol. 151, pp. 1332–1342, Mar. 2015.
[82] X.-S. Yang and S. Deb, "Engineering optimisation by cuckoo search," *Int. J. Math. Model. Numer. Optim.*, vol. 1, no. 4, pp. 330–343, 2010.
[83] D. Simon, "Biogeography-based optimization," *IEEE Trans. Evol. Comput.*, vol. 12, no. 6, pp. 702–713, Dec. 2008.
[84] N. J. Cheung, X.-M. Ding, and H.-B. Shen, "A nonhomogeneous Cuckoo search algorithm based on quantum mechanism for real parameter optimization," *IEEE Trans. Cybern.*, vol. 47, no. 2, pp. 391–402, Feb. 2017.

ASHFAQ AHMAD received the B.S. degree in mathematics from the Islamia College Peshawar, in 2015, and the M.Phil. degree in mathematics from Abdul Wali Khan University Mardan, Pakistan, in 2018, where he is currently pursuing the Ph.D. degree in mathematics. His research interests include optimization algorithms, real world problems, bio-inspired algorithms, artificial neural networks, and energy management.

MUHAMMAD SULAIMAN received the B.Sc. degree from the University of Peshawar, in 2004, the M.Sc. and M.Phil. degrees in mathematics from the Quaid-i-Azam University Islamabad, Pakistan, in 2007 and 2009, respectively, and the Ph.D. degree in mathematics from the University of Essex, U.K., in 2015. From 2009 to 2016, he was a Lecturer in mathematics with Abdul Wali Khan University Mardan, Pakistan, where he has been an Assistant Professor with the Department of Mathematics, since February 2016. He is the author of two book chapters and more than 45 research articles. His research interests include mathematical optimization techniques, global optimization, evolutionary algorithms, heuristics, metaheuristics, multi-objective optimization, design engineering optimization problems, structural engineering optimization problems, linear programming, linear and non-linear least squares optimization problems, evolutionary algorithms, nature-inspired metaheuristics, artificial neural networks, and differential equations. He is currently an Associate Editor of the journal *COJ Reviews and Research* and *SCIREA Journal of Mathematics*.

POOM KUMAM (Member, IEEE) received the Ph.D. degree in mathematics from Naresuan University, Thailand. He is currently a Full Professor with the Department of Mathematics, King Mongkut's University of Technology Thonburi (KMUTT). He is also the Head of the Fixed Point Theory and Applications Research Group, KMUTT, and the Theoretical and Computational Science Center (TaCS-Center), KMUTT. He is also the Director of the Computational and Applied Science for Smart Innovation Cluster (CLASSIC Research Cluster), KMUTT. He has authored or coauthored more than 800 international peer-reviewed journals. His main research interests include fixed point theory and applications, computational fixed point algorithms, nonlinear optimization, control theory, and optimization algorithms.

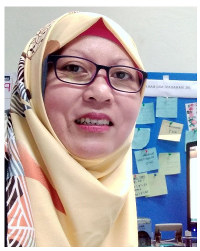

MAHARANI ABU BAKAR received the Ph.D. degree in mathematical sciences from the University of Essex, in 2015. She is currently working as a Senior Lecturer with the Department of Applied Mathematics, Universiti Malaysia Terengganu (UMT). She is also a member of the Applied Mathematics and Scientific Computing Research Interest Group, UMT. She has authored and coauthored more than 20 research articles and conference articles. Her research interests include numerical analysis and its relations with the solutions of problems, which involve large scale of variables, parallel computing, and cloud computing. Recently, she has been working on solving the high-dimensions of partial differential equations solutions by using machine learning, particularly using support vector regression (SVR) and artificial neural networks (ANNs) models.

MIFTAHUDDIN received the bachelor's degree from the University of Hasanuddin, South Sulawesi, the master's degree from Bandung Institute of Technology, West Java, and the Ph.D. degree from the University of Essex, Colchester, U.K. He is currently working as a Lecturer, a Researcher, and an Entrepreneur with the Statistics Studies Program, Department of Statistics, Faculty of Mathematics and Sciences, Syiah Kuala University, Banda Aceh. His areas of expertise are statistical modeling, machine learning, data analysis, big data, data sciences, biometrics, time series and regression analysis, semiparametric models, stochastic processes, actuarial sciences, financial analysis, and geostatistics (time-spatial). His supervisor was Prof. Berthold Lausen, the Head of Mathematical and Statistical Sciences, University of Essex.